2014

HABITABILITY OF ULTRABASIC, SERPENTINITE-ASSOCIATED WATERS FROM COAST RANGE AND PHILIPPINES OPHIOLITES

Tabetha Juliann Scott
University of Rhode Island, tjscott22@gmail.com

HABITABILITY OF ULTRABASIC, SERPENTINITE-ASSOCIATED WATERS FROM COAST RANGE AND PHILIPPINES OPHIOLITES

BY

TABETHA JULIANN SCOTT

A THESIS SUBMITTED IN PARTIAL FULFILLMENT OF THE

REQUIREMENTS FOR THE DEGREE OF

MASTER OF SCIENCE

IN

BIOLOGICAL AND ENVIRONMENTAL SCIENCES

UNIVERSITY OF RHODE ISLAND

2014

MASTER OF SCIENCE IN BIOLOGICAL AND ENVIRONMENTAL SCIENCES

OF

TABETHA JULIANN SCOTT

APPROVED:

Thesis Committee

Major Professor: Dawn Cardace

Tom Boving

Jose Amador

Nasser H. Zawia
DEAN OF THE GRADUATE SCHOOL

UNIVERSITY OF RHODE ISLAND
2014

ABSTRACT

The deep biosphere in cold, dark sub-seafloor ultramafic rocks (*i.e.*, those rocks rich in Fe and Mg) is stressed by exceedingly high pH of through-going solutions, transient, if any, inorganic carbon availability, and little known organic carbon inventories. As a test of heterotrophic carbon use, serpentinite-associated waters (from groundwater sampling wells and associated surface seepages in tectonically uplifted mantle units in ophiolites) were tested for differences with respect to aqueous geochemistry and microbial growth assays in EcoPlates™ - BioLog Inc. This work focuses on two field locations for water sampling: the Coast Range Ophiolite, CA, USA, and the Zambales Ophiolite, Philippines. Characteristics of each sampling site are presented (pH, ORP, Conductivity, temperature, lithology, %DO, depth, and Ca^{2+}/Mg^{2+} ratios). Complementary EcoPlate™ results [prefabricated 96-well plates, seeded with triplicate experiments for determining microbiological community response to difference organic carbon sources; a triplicate control experiment with no carbon source is built in to the plate] are also presented. Waters from selected California sites [7 discrete groundwater monitoring wells and 5 hydrologically connected sites] and Philippines sites [4 Zambales Ophiolite springs/seepages] sourced in serpentinites were analyzed. EcoPlate™ average well-color development (AWCD), which demonstrates microbial activities averaged per plate (as in Garland and Mills, 1991), differs across sites. Correlations of AWCD with environmental data are evaluated. Clarifying the geochemical-biological relationships that bear out in these analyses informs discourse on the energetic limits of life in

serpentinizing systems, with relevance to ultramafic-hosted life on continents and in the seabed.

ACKNOWLEDGMENTS

I would first like to extend appreciation to my major advisor, Dr. Dawn Cardace for all of the support and encouragement throughout this process, along with my lab mates Amy Stander, Ken Wilkinson, and Alex Bowman for collaboration on field work and general support. Secondly I would like to thank my committee members Drs Tom Boving and Jose Amador for their guidance. Also at the University of Rhode Island, I would like to acknowledge the support of Dr. Vinka Craver and lab (Nelson Anaya, Varun Kasaraneni, Colleen Grinham, and Farrah Solomon).

Field work at the McLaughlin Natural Reserve would not have been possible without the backing and knowledge of reserve staff, particularly reserve resident directors Paul Aigner and Cathy Koehler, and reserve steward Rhett Woerly. Collaboration with NASA AMES scientists has also been critical (Tori Hoehler, Mike Kubo, and Dan Carnevale), as has collaboration with Matt Schrenk's lab, now at Michigan State University. New Idria samples were collected in collaboration with Ryan O'Dell, Natural Resources Specialist with the BLM, Hollister Field Office. Philippines field work could not have been possible without the partnership of Dr. C. A. Arcilla at the University of the Philippines, National Institute of Geological Sciences (NIGS) and Dr. D'Arcy Meyer-Dombard at the University of Illinois, Chicago, Department of Earth and Environmental Sciences.

I would like to recognize the support and funding from the University of Rhode Island College of Environmental and Life Sciences for teaching and research assistantships, as well as funding from National Science Foundation (NSF EAR

Award 1146910) and the Rhode Island Space Grant. All have contributed to my success in completing this project.

PREFACE

This document is prepared in manuscript format and adheres to the style of the scientific journal *Geobiology*.

TABLE OF CONTENTS

LIST OF TABLES

TABLE PAGE

LIST OF FIGURES

MANUSCRIPT – 1

Prepared for publication in Geobiology Journal

Habitability of Ultrabasic, Serpentine-associated Waters from Coast Range and Philippines Ophiolites

Tabetha Juliann Scott

Biological and Environmental Sciences

University of Rhode Island, RI USA

Corresponding Author: Dawn Cardace, Ph.D.

Biological and Environmental Sciences

University of Rhode Island

334 Woodward Hall

9 East Alumni Avenue

Kingston, RI, 02881, USA

Phone: +1 (401) 874-9384

Email: Cardace@mail.uri.edu

INTRODUCTION

Earth's deep biosphere has been estimated as extensive, with a total associated biota that could rival surface microbial regimes (Gold, 1992; Whitman et al 1998), or considerably more modest estimates of associated biota (Kallmeyer et al. 2012; Jorgensen, 2012). Carbon and other element cycling in the deep biosphere are expected to be influenced by biogeochemical activities in Earth's deep sedimentary layers of the ocean floor and underlying rocks. The habitability of deep oceanic lithosphere composed of serpentinizing peridotite is still poorly understood. H_2, CH_4, and CO_2 metabolizing microbial communities in serpentinizing systems have been postulated and the role of heterotrophy is still controversial (Schrenk et al 2013).

Ophiolite sequences on continents provide access to tectonically uplifted mantle units, which in turn provide direct access to serpentinizing ultramafic units and their associated microbiological communities. Ophiolite sequences may be emplaced onto continental crust due to suprasubduction zone processes, and are often not in a predictable sequence but instead are well mixed mélange terrains. Modern deep sea vent extreme environments such as the Lost City Hydrothermal Field are similar geologically and geochemically to exposed sections in ophiolites, but are difficult to access (Kelly et al., 2005). The Coast Range Ophiolite (CRO) (Figure 1) and Zambales Ophiolite (ZO) (Figure 2) are examples of mélanges with direct access for study. Both ultramafic units are actively dewatering, producing microbe-bearing groundwaters via seeps, springs, or wells (Cardace et al., 2013, Cardace et al., 2014, in review).

The Coast Range Ophiolite is found trending roughly NW-SE in northern California from Elder Creek to Point Sal; transform faulting from the San-Andreas and Sur-Nacimiento faults have altered and cut the ultramafic unit (Shervais et al., 2005). Tectonically subjacent to the Franciscan assemblage, the CRO has easily accessible ultramafic blocks that represent the base of uplifted oceanic lithosphere (Figure 3). Origins of the Coast Range Ophiolite are still controversial but are taken to have formed through suprasubduction zone processes from extension-driven faulting in young arc rocks during the middle to late Jurassic (Shervais, et al 2005).

The Zambales Ophiolite (ZO) consists of fragments of Eocene oceanic crust that formed in proximity to an island arc (Abrajano, et al. 1988) and now occupies a fore-arc setting with respect to the Manila Trench. A large, complete, and relatively young ophiolite, the ZO is considered to be an excellent model system for the study of island arc ophiolite genesis (Schweller, et al. 1983). Multiple locations of extensively mapped ultramafic units are exposed at the surface in the Zambales region.

Assessing the habitability of ultramafic rock-hosted systems can be applicable to early life environments on Earth. Consistent sources of energy are one of the factors in determining locations for potential development of early life. Considering serpentinizing systems produce sustained chemical energy not only in the form of methane and hydrogen but also other energy sources such as minor formate and ammonia (Yi, Weijie et al 2013), microbial metabolisms may have been shaped by these systems early in the history of life on Earth life (Russell et al., 2010). Understanding the limits of life and how organisms evolve to overcome challenges

continues to be important to understanding how life might have evolved on early Earth.

Along with applicability to early life on earth, terrestrial serpentinizing systems are analogous to specific settings on other planets, and are thus relevant to astrobiology also. Serpentine has been found on the surface of Mars by the Reconnaissance Orbiter (Ehlmann et al., 2010). The presence of serpentine on Mars is significant in regards to considerations of habitability (Ehlmann, et al., 2010). Sites such as the McLaughlin Crater or the mélange terrains at the Claritas Rise and the Nili Fossae might still preserve clues to past life on mars. There is a high potential to gain a deeper understanding of early life on Earth from these sites which are approximately 3.8 Ga, roughly the same age as some of the earliest proposed evidence for life on Earth.

The purpose of this study is to improve the scientific understanding of microbial ecology in serpentinizing environments. To accomplish this, the aqueous chemistry of surface and subsurface serpentinizing systems is characterized, focusing on calcium/magnesium ratios. Calcium-dominated waters represent deeply sourced waters closed to the atmosphere, whereas magnesium-dominated waters represent shallower waters open to the atmosphere; the ratio of these cations demonstrates the mixing of these two types of waters (Neal and Stanger 1985; Paukert et al., 2012).The host rock and interactions with surface processes should determine chemistry of emanating fluids. Water chemistry and environmental parameters (pH, oxidation reduction potential, temperature, dissolved oxygen, and conductivity) of surface and subsurface waters will be considered with concurrent EcoPlate™ microbial

community assessment tests to determine factors that significantly influence community structure. Microbial communities will be evaluated using EcoPlates™; which are effective in determining a physiological profile of heterotrophic microbiological communities. Utilization of EcoPlate™ experiments is a way to measure and compare the metabolic diversity of the mixed microbial communities.

MATERIALS AND METHODS

CRO sampling sites in this study are located in the McLaughlin Natural Reserve, near Lower Lake, CA, administered by the University of California, Davis. Extensive serpentine grasslands, exposed ultramafic blocks, and groundwaters are accessed in this locale. ZO sampling sites in this study were accessed by private permission (for private lands) or formal approval (for park lands).

Water Sampling

Samples collected for inductively coupled plasma mass spectrometry (ICP-MS) are filtered with syringes (rinsed three times) fitted with 0.22 µm pore size syringe filters. ICP-MS samples are collected in pre-cleaned 100 ml bottles spiked with trace metal grade 1:1 HNO_3, for a target final concentration of ~2%HNO_3. Field chemistry parameters were measured with YSI-556 multiprobe, a handheld device used to measure water pH, temperature, conductivity (EC), dissolved oxygen (DO), and oxidation reduction potential (ORP). Unfiltered water intended for EcoPlate™ inoculations are collected with sterile syringes (surface collection) or pumped directly (subsurface collection) into new bottles; both are rinsed three times prior to use.

Subsurface waters at McLaughlin Natural Reserve (MNR), CA are sampled with a bladder pump assembly installed in wells following drilling (Aug-Dec 2011, Cardace et al., 2013). Pumps are set at a screened interval in the bottom of each well. Waters are pumped into a flow through cell connected to an YSI-556 multiprobe that measures real time changes in chemical parameters observed during pumping. In the

Philippines, surface waters from springs are collected with syringes as described above. Subsurface waters collected at Bigbiga farm, Philippines are collected from an artesian well. Tubing is inserted into the well pipe outlet to collect samples with minimal atmospheric interference.

Use of EcoPlates™

A multi-channel pipette and sterile pipette tips are used to inoculate EcoPlate™ wells with unfiltered water. Samples are pipetted from a tray that is rinsed with DI water three times and subsequently rinsed three times with sample to self-contaminate the tray. Carbon sources and redox dye do not affect pH; therefore sample pH is reflected in EcoPlate™ experiments. Plates are analyzed in an OmniLog Phenotype MicroArray System with experimental parameters set to record color intensity every 15 minutes for 72 hours at 25°C. EcoPlates™ are designed with triplicate experiments per carbon source to show variability of utilization per sample. Plates contain 93(Figure 4), 100 µL wells inoculated with 31 distinct carbon sources, nutrients and dye, and 3 control wells with only dye. Control wells are used as a reference point in which utilization of compounds in background water chemistry can be measured. Components are supplied to each well in dried-film form that is reconstituted upon sample inoculation. Carbon sources supplied in the EcoPlate™ are arbitrary and do not correspond to carbon sources in the natural environment of samples; however, they can be used to compare and contrast metabolic capabilities across samples. EcoPlates™ alone are not sufficient to determine specific microbial colonies in a mixed community sample.

Color intensity changes that are recorded are due to the redox dye tetrazolium violet which detects respiration in the form of nicotinamide adenine dinucleotide (NADH) from the utilization of carbon sources (Garland and Mills, 1991). False positives can occur in samples that have Ca^{2+}concentrations greater than 100ppm. This false positive or 'calcium effect' is the result of the inability of the water to dissolve materials in the well (Pierce et al, 2013). Undissolved materials create a film on the wells, resulting in false absorbance readings. Absorbance data for each well are normalized by averaging the triplicate color change results for each carbon source and then subtracting the average of the control well color change. This determined the average well color density (AWCD) per time point.

Average well color density is used to calculate the net area under the curve using the trapezoidal rule for calculation. This enables a direct comparison of utilization across carbon sources per sample as well as sample to sample comparison (Guckert, et al. 1996).

$$AWCD = \sum_{i-1}^{n} \left[\left(\frac{v_i + v_{i-1}}{2} \right) \times (t_i - t_{i-1}) \right]$$

v = absorbance value

t = time

Inductively Coupled Plasma Mass Spectrometry

Dissolved chemical species are analyzed on an iCAP Q inductively coupled plasma mass spectrometer (ICP-MS)**.** Samples were run at three dilutions: 1:250, 1:150, and 1:5. Samples were standardized at two percent trace metal grade HNO_3. Sample controls of 2% nitric acid standardizing solution, Inductively Coupled Plasma

– Stock Solution (ICP-SS) and a Trace Metal in Drinking Water (TMDW) solution were analyzed as accuracy checks.

Principal Component Analysis

Data are analyzed using a principal component analysis (PCA) with JMP® version 10.0.2. Correlations are used in PCA of all collected data for data comparison with scale-invariance (Glimm, et al 1997). Two methods for determining importance of parameters were used in the PCA analysis; the score plot and the vector plot. The score plot is determined by the eigenvalues, whereas the vector plot is determined by the eigenvectors.

Mineralogy of Serpentinite Substrate

Bulk powder x-ray diffraction (XRD) is applied to solid samples to confirm minerals present. Representative rock samples are collected at surface and well sites. Samples are dried and powdered using a percussion mortar, followed by selecting fines for analysis that have passed through a 150 μm sieve. Samples are then placed into the Olympus Terra XRD sample cell for analysis. Diffractogram are analyzed using XPowder software, which references published profiles for known minerals and facilitates peak identification.

RESULTS

EcoPlate™ experiments were conducted to determine if microbial metabolic fingerprints vary between serpentinizing sites. To make this determination, unfiltered waters from the sampling locations were used to inoculate EcoPlates™. Metabolic responses are driven by the carbon source in the EcoPlate™ wells. Carbon sources are categorized into six guilds: amino acids, amines and amides, carboxylic acids, carbohydrates, miscellaneous, and polymers (Table 1) (Amador and Görres, 2007). Collectively, metabolic response to carbon sources will determine the microbial metabolic fingerprint for each site (Figure 5). Sampling localities are categorized by geographic location (Coast Range Ophiolite, California and Zambales Ophiolite, Philippines) and by interaction with atmospheric conditions (surface and subsurface).

Carbon utilization patterns vary among locations. In the Coast Range Ophiolite surface and subsurface sites have distinct differences. Surface sites have an elevation-controlled gradient associated with carbon utilization; as demonstrated by fewer carbon sources utilized by collection sites further upstream than sites downstream. For instance, the community at site TC-A utilizes fewer carbon sources and is at the highest elevation, while the community at TC-E utilizes the most carbon sources out of the California surface sites, and is at the lowest elevation (Table 2). Subsurface samples have different carbon utilization patterns in comparison to surface samples. Correlations can be found in association with rock type at bore-hole termination but not with depth. For instance, CSW 1-1 is at a depth of 19.5 feet and CSW 1-4 is at a depth of 8.8 feet; both terminate in clays with serpentine gravels, both utilize the same carbon sources with the exception of N-Acetyl-D-Glucosamine. CSW 1-1 was able to

utilize it and CSW 1-4 was not (Table 3). None of the subsurface sites utilized i-Erythritol whereas all of the surface sites were able to utilize this complex carbon source. None of the California sites were able to utilize 2-Hydroxy Benzoic Acid.

Carbon utilization patterns in the Philippines samples were different from California sites. In general, surface sites utilized more carbon sources than subsurface sites (Table 4). Subsurface site ML1, ML2, and BB1 along with surface site PB1 all did not utilize β-Methyl-D-Glucoside, D-mannitol, or D-Galacturonic. ML1 and ML2 both could not utilize N-Acetyl-D-Glucosamine where other sites did. ML1 was also not able to utilize α-cyclodextrin, D-Galactonic Acid γ-Lactone, L-theonine or L-serine while other sites were able to. I-erythritol was not utilized at any site with the exception of CC1. Sites PB1 and ML2 both were not able to utilize Pyruvic Acid Methyl Ester and 4-Hydroxy Benzoic Acid, all other sites utilized these complex carbon sources. As with California, none of the Philippines sites utilized 2-Hydroxy Benzoic Acid.

Calcium and magnesium were analyzed for each water sample by ICP-MS (Table 5). Surface water sites have a Ca/Mg ratio of <1 in California. Subsurface wells and deeply sourced spring sites in both California and the Philippines have a Ca/Mg ratio >1, except for well CSW 1-4 in CA, with some shallow meteoric component, and the artesian well at Bigbiga (BB1), sourced in altered pillow basalts. The highest Ca/Mg ratios in California were found in QV 1-3, CSW 1-2, Old CSW, and QV 1-1 with Ca/Mg ratios from 19 to 99. The Philippines waters have Ca/Mg ratios of ~6 at ML1 and ML2, and the highest Ca/Mg ratio can be found at PB1 (14), though Ca/Mg drops to 0.2 downstream at PB2. None of the sampling locations had

Ca^{2+} concentrations greater than 100 ppm; therefore, the 'calcium effect' identified in the Methods section above was not a concern; we do not expect false positives in EcoPlate™ response in this study.

Environmental parameters (temperature, conductivity, dissolved oxygen, pH, and redox) were evaluated at each sampling site (Table 5). California surface locations are considered any collection site that has interaction with the atmosphere, while subsurface sites do not appear to have considerable interaction with the atmosphere. All Philippines surface sites are considered in the same fashion as CA surface sites, and all well and groundwater seeps to be 'subsurface.' BB1 waters are unique in the 'subsurface' sample set since they are sourced in mafic pillow basalts rather than ultramafic serpentinites (as at PB sites), and do not appear to be geologically near the contact between the buried gabbroic complex and ultramafics (as at ML sites).

California surface waters are warmer than subsurface waters by as much as 6.9°C. California surface waters range from 22.2°C to 23.8°C; while subsurface waters range from 16.6°C to 22.1°C (Table 5). Philippines sites have warmer temperatures ranging from 26.4°C at the Poon Bato River to 34.4°C in sampling sites ML1 and ML2.

Conductivity and dissolved oxygen reading follow similar patterns across sites (Table 5). California surface waters have conductivity reading ranging from 3.53 to 5.72 mS/cm. Subsurface California waters are somewhat similar to surface waters ranging from 1.7 to 5.09 mS/cm, with the exception of Old CSW which had a conductivity reading at 11.34 mS/cm, likely due to leakage of saline components from nearby marine sedimentary units. Philippines conductivity readings were considerably

lower than California ranging from 0.17 to 0.45 mS/cm across all sites. Dissolved oxygen is higher in California surface sites (19.3 – 24%) in comparison to subsurface sites (0.5 – 6.8%). Philippines sites have a considerably lower percent DO collectively; expressions range from 0.01 – 0.9%.

The pH ranges from near neutral to very alkaline (Table 5). California surface sites range from 8.3 to 8.6; subsurface sites vary from 7.8 – 12.2. Philippines sites consistently have similar pH values (9.2 – 10.9). Lower pH values are encountered at sites mixing with freshwater sources (PB2 and Poon Bato River).

Oxidation reduction potential (ORP) is negative for all sites (Table 5). California surface sites (-19 to -29 mv) are more oxidizing/less reducing than subsurface sites (-23 to -295 mv) as a whole; while Philippines sites are more reducing as a whole than California sites, ranging from (-97 to -460 mv). Sites in the Philippines do not exhibit a distinctive pattern in ORP data between surface sites to subsurface sites.

At the McLaughlin Natural Reserve, CA, CRO subsurface sites were sampled at nine different locations at different depths and terminate in different lithology. CSW 1-1 and 1-2 wells are drilled to approximately 19 m, terminating in clays and serpentinite gravel. CSW 1-3 and QV 1-1 wells are drilled to a depth of approximately 22 m, terminating in serpentine-rich altered mafic rocks and magnetite-bearing clays with albite (likely altered basalts). CSW 1-4 is drilled to a depth of approximately 7m, terminating in similar rocks of mafic-ultramafic character, and CSW 1-5 is drilled to a depth of approximately 27 m, terminating in altered mafic rock. Old CSW, which was drilled during a separate MNR project, reaches deeper than 30 m, terminating in

altered mafic rock described as gray-green clay-rich mud. Finally, QV 1-3 is drilled to a depth of approximately 35 m, terminating in albite-quartz-chlorite rich rock (likely meta-basalt). Note that all of the CSW rock types are based off of core samples that were taken from CSW 1-1; all wells are within 5 m of this well. Rock types at the QV sites are based off of core samples taken from QV 1-; associated wells are within 3 meters of this well.

Philippines surface samples flow over travertine deposits (PB1, PB2, CC1, and CC2). Subsurface waters are thought to be sourced from at least 30 m below surface in altered pillow basalts (BB1) and gabbros (ML1 and ML2). The country rock that hosts these sites is inferred from the mapped ophiolitic mélange units and structural relationships (Aurelio and Pena, 2010).

DISCUSSION

This study investigates differences in heterotrophic microbial communities in aqueous samples collected from two different serpentinizing systems hosted in the ultramafic rocks of California's Coast Range Ophiolite and the Zambales Ophiolite in the Philippines. Autotrophy may be important in these systems, but due to (i) the limited supply of dissolved organic carbon (DIC), which has largely been below detection in these hydroxide-dominated waters, and (ii) the anticipated presences of formate, acetate, and other organic compounds produced abiotically by serpentinization, heterotrophy was assessed.

While both field locations are in ultramafic units of ophiolites, tectonic histories do differ, and the ultramafics are weathering under different climate condition: older CRO rocks are in a relatively arid, low rainfall, Mediterranean-type climate and the younger ZO rocks are in a wet tropical climate with increasing monsoon seasons (Loo et al., 2014)

Olivine ((Mg, Fe) SiO_4) and pyroxenes ((Ca, Na, Fe, Mg) $(Si, Al)_2 O_6$) are minerals that dominate the mineralogy of ultramafic, Fe- and Mg- rich rocks (mantle peridotites). In ophiolites, these minerals are also found in pillow basalts and gabbros. At great depth, ultramafic mantle minerals are stable, but near surface conditions, aqueous weathering reactions render them unstable. The resulting secondary minerals (serpentine group minerals, brucite, diverse clays) are stable at low temperature and pressure, and are prominent mineralogical features in modern serpentinites. When present, relic olivines are often fragmented and interspersed with secondary minerals, largely serpentine.

Serpentine forms during olivine hydration, with resultant hydrogen production – a strong driver of microbial metabolisms--in many settings (reaction 1).

$Fe_2SiO_4 + 5Mg_2SiO_4 + 9H_2O \rightarrow 3Mg_3Si_2O_5(OH)_4 + Mg(OH)_2 + 2Fe(OH)_2$ (1)

Fayalite + forsterite + water → serpentine + brucite + iron hydroxide

Iron hydroxide is a product of olivine hydration, which can then further be reacted to produce an abiotic source of hydrogen (reaction 2).

$3Fe(OH)_2 \rightarrow Fe_3O_4 + 2H_2O + H_2$ (2)

Iron(II) hydroxide → magnetite + water + hydrogen

Chemoautotrophic metabolisms such as methanogenesis and other hydrogen-related processes require hydrogen as an energy source (Schulte et al, 2006). Naturally occurring sources of carbon in these systems could be formed abiogenically by the Fischer- Tropsch type synthesis reactions (Morrill et al., 2013). Surface/near surface waters could have residual influxes of carbon from the soils from which the water has previously infiltrated, indirectly linking the hydrology to atmospheric CO2.

Serpentinite-associated waters may mix with meteorically derived shallow ground water escaping at natural seeps. Shallow Mg^{2+}-HCO_3^- waters, Type I waters (Barnes et al., 1967; Barnes et al., 1969; Barnes et al., 1972; Barnes et al., 1978; Paukert et al., 2012; Neal and Stanger, 1985) react with soil systems open to CO_2 in the atmosphere; deeply sourced Ca^{2+}-OH^- waters, Type II waters (Barnes et al., 1967; Barnes et al., 1969, 1972, 1978; Paukert et al., 2012; Neal and Stanger, 1985) develop in ultramafic subsurface closed to the atmosphere. Mixed Type I and Type II waters results in waters of moderate pH (Cardace et al, 2011). However, some environments expressing largely Type II waters have resulting waters of pH 11 or greater (Cardace,

2010); these high pH waters are rich in Ca^{2+}, OH^-, have strongly reducing (very negative) ORP values, and high loads of dissolved hydrogen and methane similar to peridotite-hosted deep sea vents with comparable characteristics, such as the Lost City Hydrothermal Field (Kelley et al., 2001, 2005).

Coast Range Ophiolite surface water samples collected at Temptation Creek have moderate pH values (8.1 to 8.6) and small Ca/Mg ratios (0.13 to 0.20) that reveal an Mg^{2+} dominated cation inventory due to the predominance of Type II waters in surface creek flow. Surface waters interact with atmospheric gases (carbon dioxide) to develop possibly intercalated calcite-magnesium travertine deposits with banding and colored strata evident in the travertine layers. Upstream of the travertine deposits, the creek is intermittent with no significant amount of carbonate precipitation. It is likely faults/fractures release Type I groundwater into Temptation Creek as springs emerging at locations of carbonate precipitation and mixing with creek flow.

Subsurface CRO well water samples are basic to ultrabasic, with pH reaching 12.2. Sources of subsurface water in and near CRO may be old (Cretaceous) trapped sea water mixed with younger meteoric water (Peters, 1993). In the Philippines, waters likely began as a mixture also of old trapped seawater and relatively recent meteoric water, although data are sparse and unpublished on this topic (Cardace Lab, unpublished).

Levels of calcium and magnesium in fluids from sampling sites were interpreted as a function of pH (Figure 6). Temptation Creek, CA samples have the lowest Ca/Mg ratios and near neutral pH with CSW 1-4 corresponding closely to these sites. The relation is most likely due to the shallow depth (8.8 m) of CSW 1-4 well

indicating Type I water inputs. Quarry Valley wells increase in Ca/Mg ratio with increasing depth, however pH doesn't correspond to the increase in Ca/Mg ratio; QV 1-1 has the highest pH measured in all sites but a Ca/Mg ratio of only 6.64. Mixing proportions of Type I and Type II waters seem to be reflected in Ca/Mg ratios and correspond with broad shifts in pH. But given that every unit of pH increase or decrease is an order of magnitude shift in αH^+, the relationship is not linear.

The depth and relationship with lithology at the termination of the borehole strongly correlate with environmental parameters observed and microbial metabolic fingerprinting. The rocks present at water sources affect the microbial communities present in the water samples, in that they impact also the ambient aqueous geochemistry. Carbon compounds in alkaline environments may degrade in unique ways in comparison to neutral pH environments allowing for a higher degree of bioavailability. All of the CRO subsurface wells terminate in slightly different rock types (mafic to ultramafic, likely with different degrees of fault gouge processing of meta-basalt and serpentinite country rock) with different values for pH, ORP, DO, etc., revealing either different proportions of Type II water inputs or infiltration of a different subsurface hydrological regime. Similarly, ZO sites also have shifting proportions of Type I and II waters; from which different microbial fingerprints can be anticipated across sites.

Temptation Creek sites represent a Type I water-dominated system; although downstream sites may be influenced by Type II seepages. Temptation Creek site E is at the base of the creek and it has more microbial mat development than any of the upstream sites. CSW 1-4 behaves similar to the Temptation Creek samples most likely

because it is of shallow depth (8.8 m) and appears to have increases influences of Type I water also. California subsurface sites are harder to categorize. Each well has different defining characteristics (Table 5) resulting in different mixing proportions of Type I and Type II waters and correspondingly distinctive metabolic fingerprinting. Philippines sample sites are loosely correlated to sampling location. At sites CC1 and CC2 carbon utilization is very similar, as would be expected considering the environmental parameters are also nearly identical and these sites are within 10 m of each other. Sites ML1 and ML2 are considered to be sourced from the same host rock (ML1 is a gas bubbling spring source; ML2 is along a travertine rim about 150 m away, emerging from beneath vegetation), also exhibited similar carbon utilization patterns. The other surface location (PB1) is a travertine deposit forming at a fault-controlled spring alongside the large volume Poon Bato River; PB1 is more closely related to ML2 than any other site, which might indicate it is sourced in a similar serpentinizing environment. Bigbiga Spring is the only site that was sampled in the Philippines that is sourced in presumed pillow basalts; this site has distinctly different environmental parameters than any of the other sites. However, carbon utilization patterns were not significantly different from the other subsurface sites in the Philippines.

A principal component analysis (PCA) was conducted to visualize the structure of the relationships between carbon utilization patterns (*i.e.*, a representation for heterotrophic metabolic extent) and how communities are separated. The PCA is based on carbon utilization and environmental parameters (Figure 8) as well as on both sets of data combined (Figure 9). Principal component analysis on the carbon

sources is 61.9% explained by principal component 1 and 16.6% is explained by the second principal component. Vector analysis of carbon utilization (Figure 7) shows that all carbon sources except 2-hydroxy benzoic acid are positive in relation to principal component 1.

Categories of guilds tend to group together in a PCA analysis. Amino acids are clustered together mostly in quadrant I with a negative trending slope. Carbohydrates are clustered together in quadrant IV with a positive trending slope. Amines and amides are grouped in quadrant I with very little slope. Miscellaneous carbon sources all have a similar positive principal component 1 but a varied principal component 2. Most variation in carbon utilization occurs with carboxylic acids in which no clear pattern is observed. Polymers all cluster in quadrant I with a negative trending slope. According to these patterns amino acids, amines and amides, and polymers are utilized similarly; carbohydrates, most carboxylic acids, and miscellaneous carbon sources are utilized similarly. The score plot related to the carbon source PCA shows a tight clustering of most samples with the exception of two Philippines surface sites (CC2, PB1) and a quasi-subsurface Philippines site (ML1) (Figure 10).

Principal component analysis on environmental parameters (pH, ORP, %DO, conductivity, temperature, and Ca/Mg ratio) do not show clustering; only 33.6% of the data is explained in PC1 and 26.9% in PC2 (Figure 8). Conductivity and Ca/Mg fall within quadrant I and oxidation reduction potential and %DO fall within quadrant II. Temperature is in quadrant II and pH is in quadrant IV. The score plot is just as loosely correlated (Figure 11). However, Philippines sites cluster together and all surface sites in California cluster together suggesting a metabolic biogeography.

California subsurface sites cluster together with the exception of CSW 1-4 and QV1-2. This indicates that similar chemistries will group together in the PCA score plot, indicating that variation in chemistry is significantly important to the observed metabolic capacity of the sampled waters.

When combined with carbon sources, environmental parameters fall within two quadrants in the vector plot in quadrant IV (ORP, %DO, conductivity, and Ca/Mg) and in quadrant II (temperature, pH) (Figure 9). Carbon sources also demonstrate a shift in structure. Amines and amides, polymers and amino acids shifted to quadrant IV; while carbohydrates, most carboxylic acids and miscellaneous carbon sources shifted to quadrant I. The score plot yields shifted locations for some of the Philippines sites, but all other sites still cluster in a similar pattern as to the PCA on just carbon sources (Figure 12). Shifts in data structures indicate an interconnected behavior of environmental parameters and the resulting carbon utilization.

CONCLUSION

EcoPlate™ experiments show that microbiological communities from serpentinizing systems utilize carbon sources in different ways, revealing geographically distinct heterotrophic capabilities. Aqueous geochemistry and lithological context are important factors that contribute to microbial communities and thereby metabolic potential. Mixtures of Type I and II waters in California surface and subsurface sites appear to drive differing microbial metabolic profiles; proportions of Type I and II waters shift as samples tap shallow to deep groundwater flow regimes, and the changing geochemistry shapes different aqueous environments/habitats available to microorganisms. Although preliminary, data show strong correlations between microbial metabolic frameworks at the community level and observed environmental parameters, indicating that aqueous geochemistry exerts a strong influence on microbial metabolic strategies in these systems.

REFERENCES

Abrajano, TA, et al. "Methane-Hydrogen Gas Seeps, Zambales Ophiolite, Philippines: Deep or Shallow Origin?" *Chemical Geology* 71.1 (1988): 211-222.

Amador, Jose A. and Josef H. Görres. "Microbiological Characterization of the Structures Built by Earthworms and Ants in an Agricultural Field." *Soil Biology and Biochemistry* 39.8 (2007): 2070-2077.

Aurelio, M.A., Pena, R.E. "Geology of the Philippines." *Quezon City, Philippines: Mines and Geosciences Bureau* (2010).

Barnes, Ivan and JAMES R. O'NEIL. "The Relationship between Fluids in some Fresh Alpine-Type Ultramafics and Possible Modern Serpentinization, Western United States." *Geological Society of America Bulletin* 80.10 (1969): 1947-1960.

Barnes, Ivan, et al. "Metamorphic Assemblages and the Direction of Flow of Metamorphic Fluids in Four Instances of Serpentinization." *Contributions to Mineralogy and Petrology* 35.3 (1972): 263-276.

Barnes, I., V. C. Lamarche Jr and G. Himmelberg. "Geochemical Evidence of Present-Day Serpentinization." *Science (New York, N.Y.)* 156.3776 (1967): 830-832.

Barnes, Ivan, J. R. O'Neil and J. J. Trescases. "Present Day Serpentinization in New Caledonia, Oman and Yugoslavia." *Geochimica et Cosmochimica Acta* 42.1 (1978): 144-145.

Best, Myron G. *Igneous and Metamorphic Petrology.* : John Wiley & Sons, 2009.

Cardace, D., et al. "Establishment of the Coast Range Ophiolite Microbial Observatory (CROMO): Drilling Objectives and Preliminary Outcomes." *Scientific Drilling* 16 (2013): 45-55.

D. Cardace, T. M. Hoehler. "Extremophiles in Serpentinizing Systems: Implications for Life on the Early Earth and Other Planets." Ed. Susan Harrison and Nishanta Rajakaruna. *Serpentine: A Model for Evolution and Ecology.* University of California Press, 2011.

D. Cardace, T. M. Hoehler. "Subsurface Investigations of the Coast Range Ophiolite, Northern California: Field Campaign Findings." (2010).

D.Cardace, D.R, Meyer-Dombard, K.M. Woycheese and C.A. Arcilla. "Feasible Metabolic Schema Associated with High pH Springs in the Philippines." *Frontiers in Microbiology*. Portals to the Deep Biosphere (In Review).

Deschamps, Fabien, et al. "Serpentinites Act as Sponges for fluid-mobile Elements in Abyssal and Subduction Zone Environments." *Terra Nova* 23.3 (2011): 171-178.

Ehlmann, BL, JF Mustard and SL Murchie. "Geologic Setting of Serpentine Deposits on Mars." *Geophysical Research Letters* 37.6 (2010).

Fryer, Patricia. "Serpentinite Mud Volcanism: Observations, Processes, and Implications." *Annual review of marine science* 4 (2012): 345-373.

Garland, Jay L. "Analysis and Interpretation of community-level Physiological Profiles in Microbial Ecology." *FEMS microbiology ecology* 24.4 (1997): 289-300.

Garland, J. L. and A. L. Mills. "Classification and Characterization of Heterotrophic Microbial Communities on the Basis of Patterns of Community-Level Sole-Carbon-Source Utilization." *Applied and Environmental Microbiology* 57.8 (1991): 2351-2359.

Glimm, Ekkehard, et al. "Statistical Comparisons of Community Catabolic Profiles." *Journal of microbiological methods* 30.1 (1997): 71-80.

Gold, T. "The Deep, Hot Biosphere." *Proceedings of the National Academy of Sciences of the United States of America* 89.13 (1992): 6045-6049.

Guckert, James B., et al. "Community Analysis by Biolog: Curve Integration for Statistical Analysis of Activated Sludge Microbial Habitats." *Journal of microbiological methods* 27.2 (1996): 183-197.

Hackett, Christine A. and Bryan S. Griffiths. "Statistical Analysis of the Time-Course of Biolog Substrate Utilization." *Journal of microbiological methods* 30.1 (1997): 63-69.

Hopson, Clifford A. and Emile A. Pessagno Jr. "Tehama-Colusa Serpentinite Mélange: A Remnant of Franciscan Jurassic Oceanic Lithosphere, Northern California." *International Geology Review* 47.1 (2005): 65-100.

Jorgensen, B. B. "Shrinking Majority of the Deep Biosphere." *Proceedings of the National Academy of Sciences of the United States of America* 109.40 (2012): 15976-15977.

Kallmeyer, J., et al. "Global Distribution of Microbial Abundance and Biomass in Subseafloor Sediment." *Proceedings of the National Academy of Sciences of the United States of America* 109.40 (2012): 16213-16216.

Kelley, D. S., et al. "The Lost City Hydrothermal Field Revisited." *OCEANOGRAPHY-WASHINGTON DC-OCEANOGRAPHY SOCIETY*- 20.4 (2007): 90.

Kelley, D. S. "A Serpentinite-Hosted Ecosystem: The Lost City Hydrothermal Field." *Science (New York, N.Y.)* 307.5714 (2005): 1428-1434. *WOS.*

Works Cited

Loo, Yen Yi, Lawal Billa and Ajit Singh. "Effect of Climate Change on Seasonal Monsoon in Asia and its Impact on the Variability of Monsoon Rainfall in Southeast Asia." *Geoscience Frontiers*, 2014.

Madigan, Michael T., et al. *Biology of Microorganisms.* : prentice hall Upper Saddle River, NJ, 1997.

Michalski, Joseph R., et al. "Groundwater Activity on Mars and Implications for a Deep Biosphere." *Nature Geoscience* 6.2 (2013): 133-138.

Moody, Judith B. "Serpentinization: A Review." *Lithos* 9.2 (1976): 125-138.

Morrill, Penny L., et al. "Geochemistry and Geobiology of a Present-Day Serpentinization Site in California: The Cedars." *Geochimica et Cosmochimica Acta* 109 (2013): 222-240.

Neal C., Stanger G. "Past and Present Serpentinization of Ultramafic Rocks: An Example from the Semail Ophiolite Nappe of Northern Oman." *Springer Netherlands* (1985): 249-275.

Paukert, Amelia N., et al. "Reaction Path Modeling of Enhanced< i> in situ</i> CO< Sub> 2</sub> Mineralization for Carbon Sequestration in the Peridotite of the Samail Ophiolite, Sultanate of Oman." *Chemical Geology* 330 (2012): 86-100.

Peters, E. Kirsten. "D-18O Enriched Waters of the Coast Range Mountains, Northern California: Connate and Ore-Forming Fluids." *Geochimica et Cosmochimica Acta* 57 (1993): 1093-1104.

Pierce, Melissa L., J. Evan Ward and Fred C. Dobbs. "False Positives in Biolog EcoPlates< Sup> TM</sup> and MT2 MicroPlates< Sup> TM</sup> Caused by Calcium." *Journal of microbiological methods* 97 (2014): 20-24.

Russell, MJ, AJ Hall and W. Martin. "Serpentinization as a Source of Energy at the Origin of Life." *Geobiology* 8.5 (2010): 355-371.

Schrenk, Matthew O., William J. Brazelton and Susan Q. Lang. "Serpentinization, Carbon, and Deep Life." *Rev Mineral Geochem* 75 (2013): 575-606.

Schrenk, Matthew O. "Microbial Provinces in the Subseafloor." *Annual review of marine science* (2010): 279-304. *WOS.*

Schulte, Mitch, et al. "Serpentinization and its Implications for Life on the Early Earth and Mars." *Astrobiology* 6.2 (2006): 364-376.

Schulze-Makuch, D., A. G. Fairén and A. F. Davila. "The Case for Life on Mars." *International Journal of Astrobiology* 7.2 (2008): 117.

Schweller, WJ, DE Karig and SB Bachman. "Original Setting and Emplacement History of the Zambales Ophiolite, Luzon, Phillipines, from Stratigraphic Evidence." *The Tectonic and Geologic Evolution of Southeast Asian Seas and Islands: Part 2* (1983): 124-138.

Shervais, John W., et al. "Radioisotopic and Biostratigraphic Age Relations in the Coast Range Ophiolite, Northern California: Implications for the Tectonic Evolution of the Western Cordillera." *Geological Society of America Bulletin* 117.5-6 (2005): 633-653.

Sleep, N. H., D. K. Bird and E. C. Pope. "Serpentinite and the Dawn of Life." *Philosophical transactions of the Royal Society of London. Series B, Biological sciences* 366.1580 (2011): 2857-2869.

Van Baalen, MR, et al. "Environmental Geology of Belvidere Mt." (2009).

Whitman, W. B., D. C. Coleman and W. J. Wiebe. "Prokaryotes: The Unseen Majority." *Proceedings of the National Academy of Sciences of the United States of America* 95.12 (1998): 6578-6583.

Figures and Tables

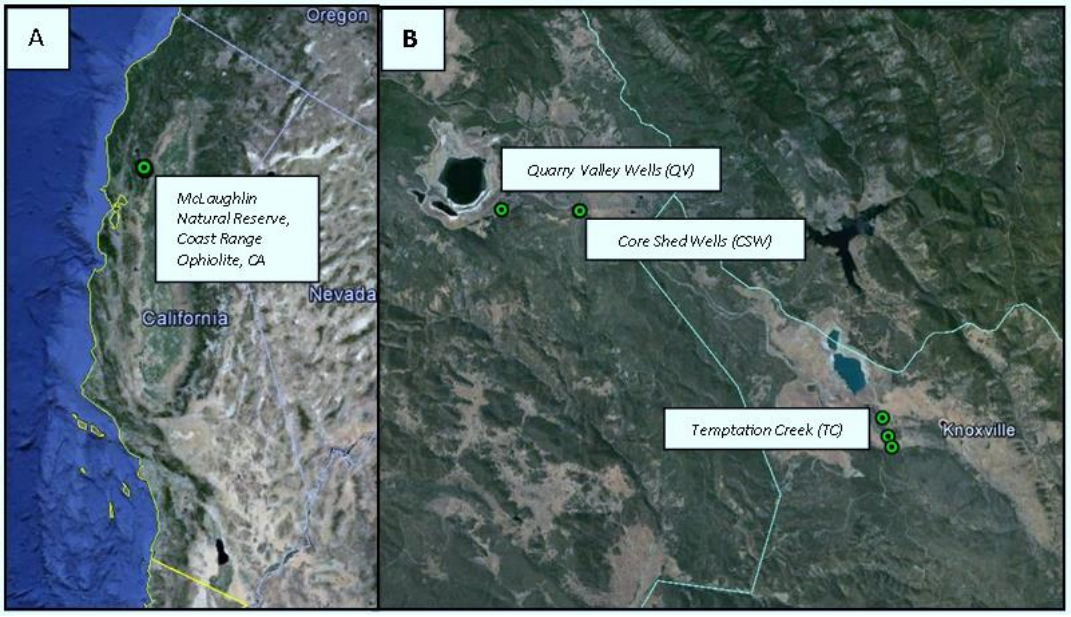

Figure 1. A) California sampling sites at the McLaughlin Natural Reserve, a research and education preserve administered by the University of California, Davis. The reserve is about 3 hours northeast of San Francisco, CA. B) Three separate collection regions within MNR, including Quarry Valley Wells (named for historic quarrying of shale beds in the vicinity), Core Shed Wells (named for the nearby regional core archive structure), and Temptation Creek (named for a seasonally active groundwater-fed creek sourced in serpentine soils).

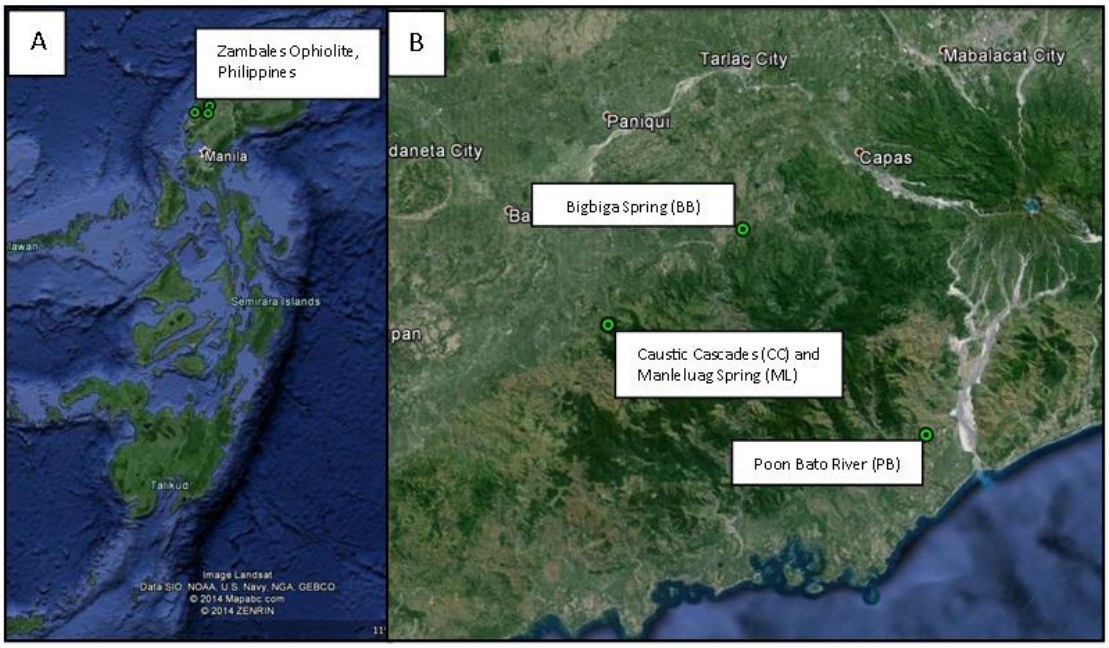

Figure 2. Philippines sampling sites, Zambales Ophiolite. Including Bigbiga Spring, Caustic Cascades/Manleluag Spring, and Poon Bato River sites.

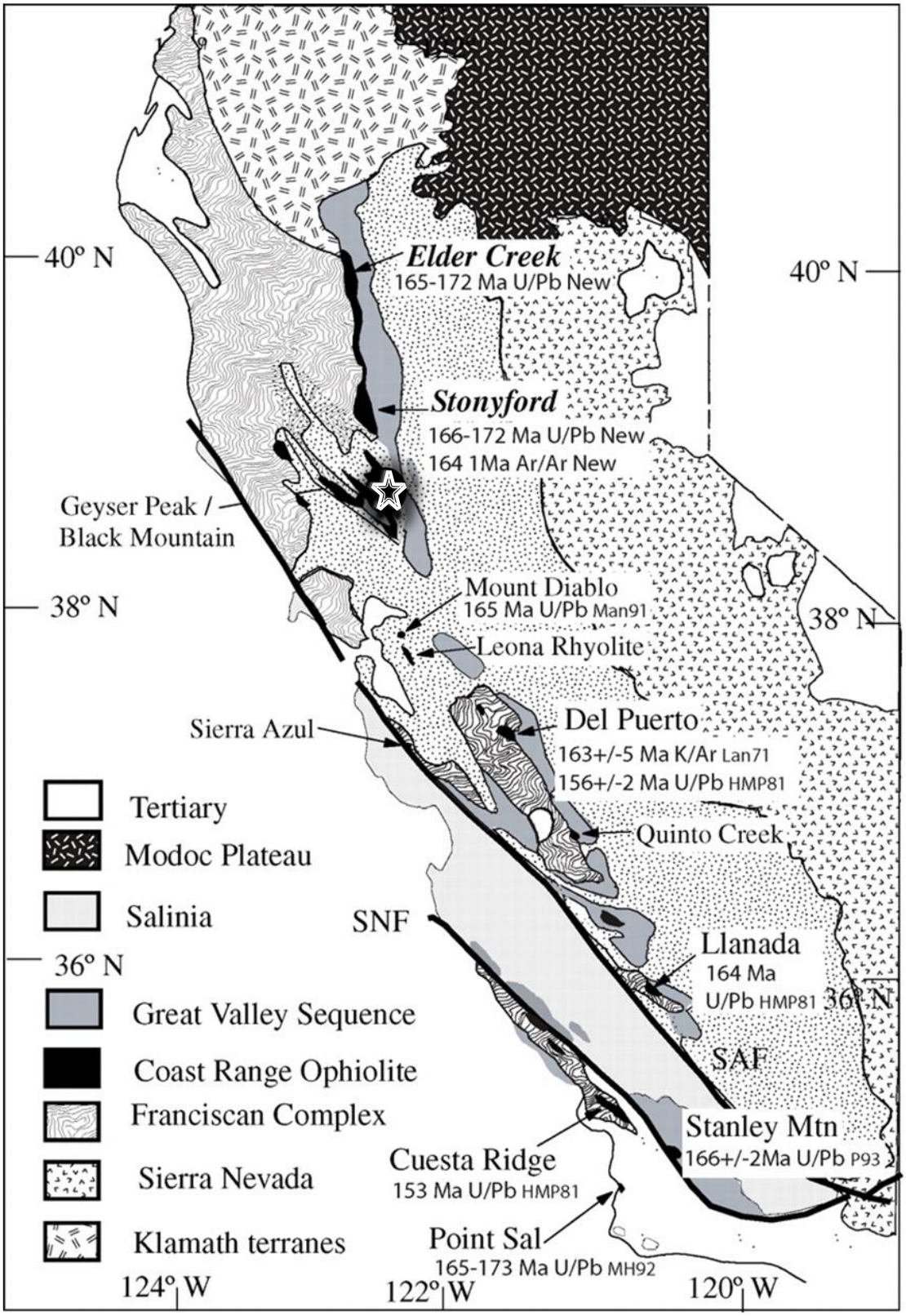

Figure 3. Geologic map of the Coast Range Ophiolite blocks, with white star indicating the MNR locality (modified from Shervais et al., 2005).

A1 Water	A2 β-Methyl-D-Glucoside	A3 D-Galactonic Acid γ-Lactone	A4 L-Arginine	A1 Water	A2 β-Methyl-D-Glucoside	A3 D-Galactonic Acid γ-Lactone	A4 L-Arginine	A1 Water	A2 β-Methyl-D-Glucoside	A3 D-Galactonic Acid γ-Lactone	A4 L-Arginine
B1 Pyruvic Acid Methyl Ester	B2 D-Xylose	B3 D-Galacturonic Acid	B4 L-Asparagine	B1 Pyruvic Acid Methyl Ester	B2 D-Xylose	B3 D-Galacturonic Acid	B4 L-Asparagine	B1 Pyruvic Acid Methyl Ester	B2 D-Xylose	B3 D-Galacturonic Acid	B4 L-Asparagine
C1 Tween 40	C2 i-Erythritol	C3 2-Hydroxy Benzoic Acid	C4 L-Phenylalanine	C1 Tween 40	C2 i-Erythritol	C3 2-Hydroxy Benzoic Acid	C4 L-Phenylalanine	C1 Tween 40	C2 i-Erythritol	C3 2-Hydroxy Benzoic Acid	C4 L-Phenylalanine
D1 Tween 80	D2 D-Mannitol	D3 4-Hydroxy Benzoic Acid	D4 L-Serine	D1 Tween 80	D2 D-Mannitol	D3 4-Hydroxy Benzoic Acid	D4 L-Serine	D1 Tween 80	D2 D-Mannitol	D3 4-Hydroxy Benzoic Acid	D4 L-Serine
E1 α-Cyclodextrin	E2 N-Acetyl-D-Glucosamine	E3 γ-Hydroxybutyric Acid	E4 L-Threonine	E1 α-Cyclodextrin	E2 N-Acetyl-D-Glucosamine	E3 γ-Hydroxybutyric Acid	E4 L-Threonine	E1 α-Cyclodextrin	E2 N-Acetyl-D-Glucosamine	E3 γ-Hydroxybutyric Acid	E4 L-Threonine
F1 Glycogen	F2 D-Glucosaminic Acid	F3 Itaconic Acid	F4 Glycyl-L-Glutamic Acid	F1 Glycogen	F2 D-Glucosaminic Acid	F3 Itaconic Acid	F4 Glycyl-L-Glutamic Acid	F1 Glycogen	F2 D-Glucosaminic Acid	F3 Itaconic Acid	F4 Glycyl-L-Glutamic Acid
G1 D-Cellobiose	G2 Glucose-1-Phosphate	G3 α-Ketobutyric Acid	G4 Phenylethyl-amine	G1 D-Cellobiose	G2 Glucose-1-Phosphate	G3 α-Ketobutyric Acid	G4 Phenylethyl-amine	G1 D-Cellobiose	G2 Glucose-1-Phosphate	G3 α-Ketobutyric Acid	G4 Phenylethyl-amine
H1 α-D-Lactose	H2 D,L-α-Glycerol Phosphate	H3 D-Malic Acid	H4 Putrescine	H1 α-D-Lactose	H2 D,L-α-Glycerol Phosphate	H3 D-Malic Acid	H4 Putrescine	H1 α-D-Lactose	H2 D,L-α-Glycerol Phosphate	H3 D-Malic Acid	H4 Putrescine

Figure 4. EcoPlate™ carbon sources as presented for experiments. 96 well plates contain 31 unique carbon sources replicated in triplicate to evaluate consistency. A control well that is devoid of any carbon source acts as a reference well to determine how well a carbon source is utilized.

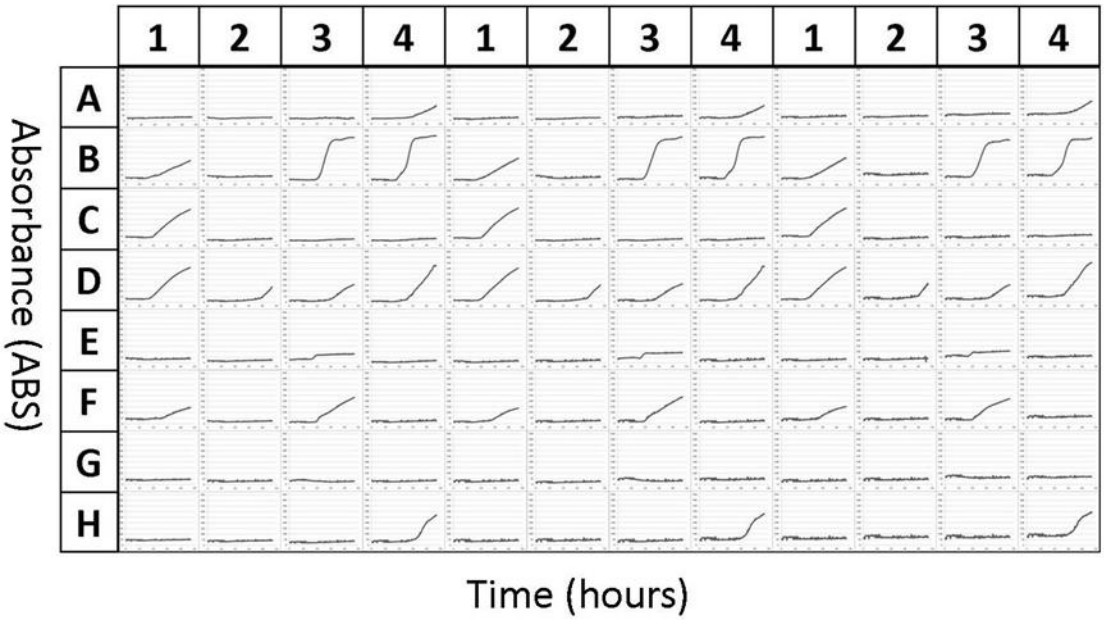

Figure 5. OmniLog color absorbance readings versus time for each carbon source. As a representative experiment, for this inoculant, wells 4-B shows utilization of a carbon source with characteristic phases of growth. Lag phase is the initial period of time in which cells are acclimating to the environment, 0 – 15 hours in this instance. Exponential growth phase is the time period in which cells grow at an exponential rate (15 – 30 hours). Deceleration phase is the time period when essential nutrients are depleted and toxins that are produced are accumulating (30 – 35 hours). Stationary phase is the time period in which net cell growth is about zero (35 – 48 hours) (Madigan et al., 1997).

Guild	Substrate	Well no.
Amino acids	L-arginine	A4
	L-asparagine	B4
	L-phenylalanine	C4
	L-serine	D4
	L-threonine	E4
Amines and amides	Phenylethylamine	G4
	Putrescine	H4
Carboxylic acids	D-galactonic acid γ-lactone	A3
	D-galacturonic acid	B3
	2-hydroxybenzoic acid	C3
	4-hydroxybenzoic acid	D3
	γ-hydroxybutyric acid	E3
	D-glucosaminic acid	F2
	Itaconic acid	F3
	Glycyl-L-glutamic acid	F4
	α-ketobutyric acid	G3
	D-malic acid	H3
Carbohydrates	β-methyl-D-glucosamine	A2
	D-Xylose	B2
	i-erythritol	C2
	D-mannitol	D2
	N-acetyl-D-glucosamine	E2
	D-cellobiose	G1
	α-D-lactose	H1
Miscellaneous	Pyruvic acid methyl ester	B1
	Glucose-1-phosphate	G2
	D,L-α-glycerol phosphate	H2
Polymers	Tween 40	C1
	Tween 80	D1
	α-cyclodextrin	E1
	Glycogen	F1

Table 1. Guild groupings of carbon substrates used in BioLog EcoPlate™ experiments with well numbers. (Amador and Görres, 2007)

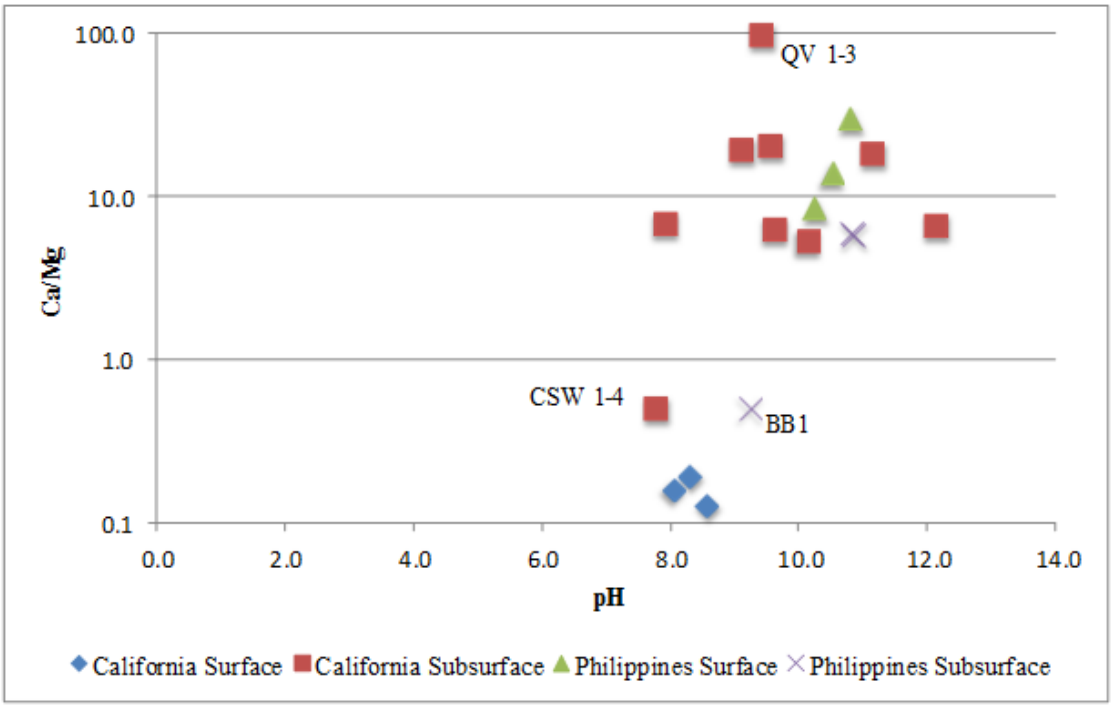

Figure 6. Calcium to magnesium ratios across sites. Ratios correspond closely not only to depth relationships but also other factors. Surface sites in California group together and are closely related to CSW 1-4, which is located at a depth of 8.8 m below surface. California subsurface sites vary considerably and other factors besides depth are contributing to calcium levels. Philippines surface sites group closely and are within the same magnitude. Philippines subsurface sites ML1 and ML2 are nearly identical indicating similar water sources (possibly gabbros); while BB1 clearly is originating from a different source (coring data suggest altered pillow basalts).

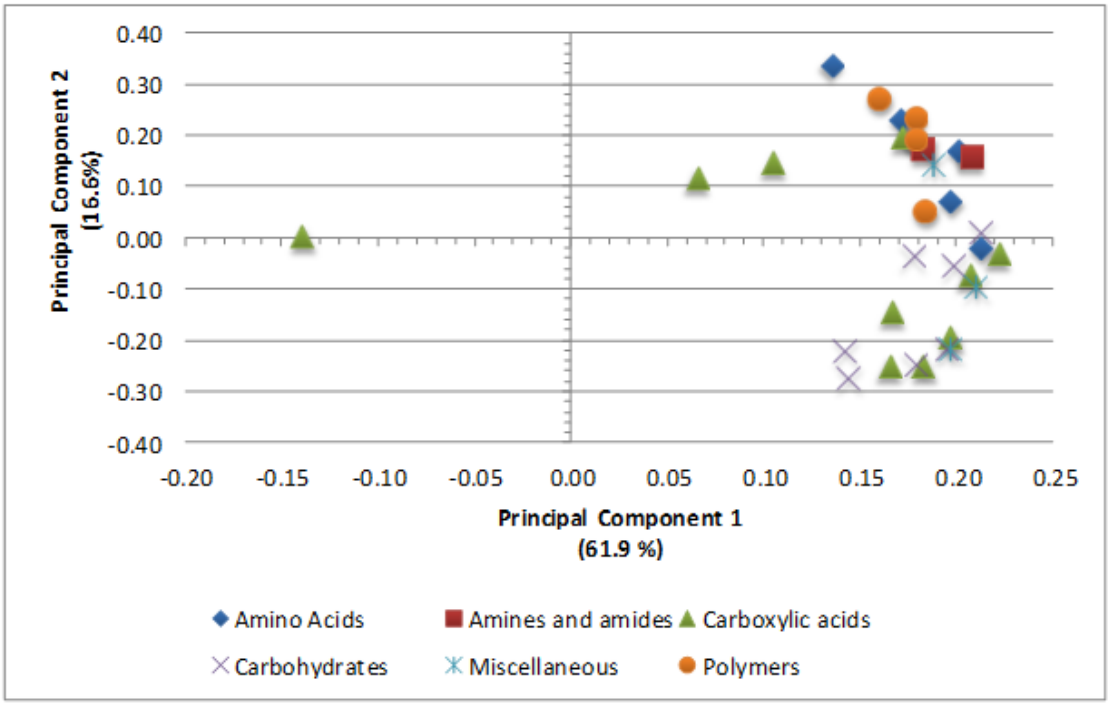

Figure 7. Vector plot of principal component analysis based on carbon utilization of all water samples.

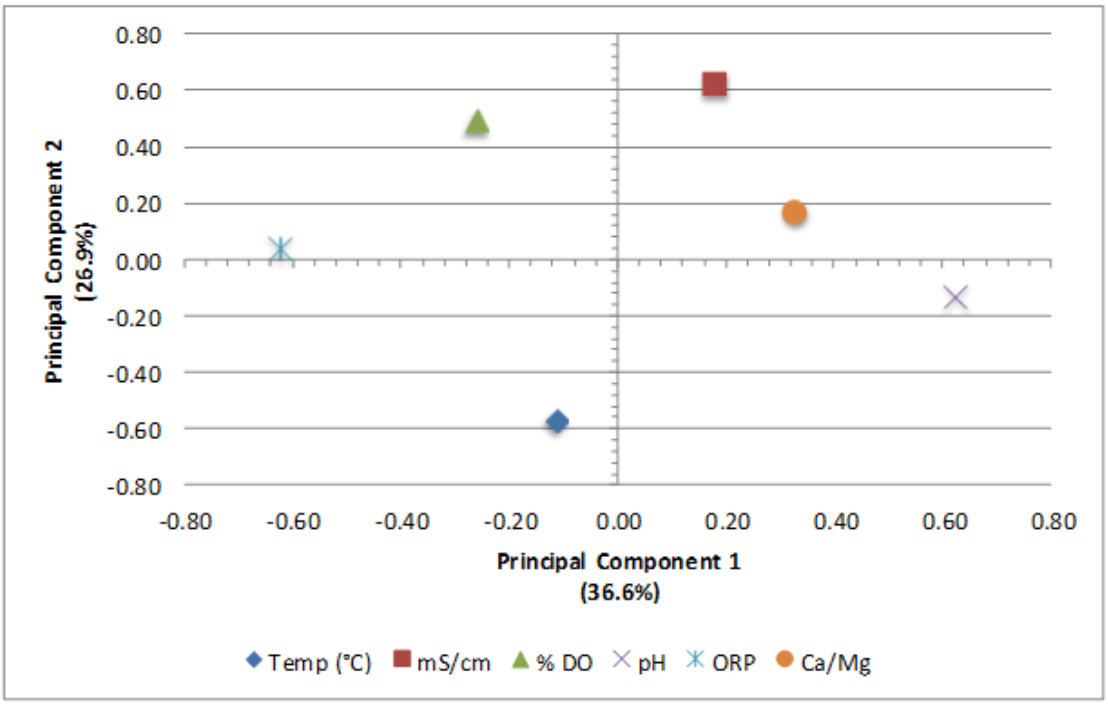

Figure 8. Vector plot of principal component analysis of the environmental parameters of all water samples.

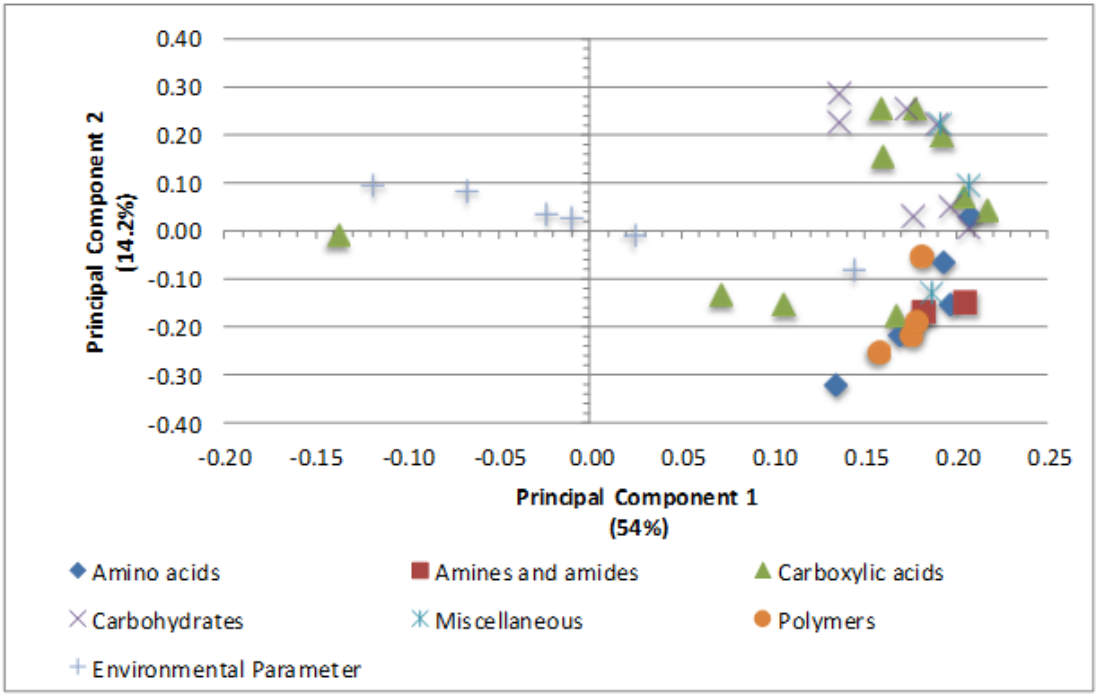

Figure 9. Vector plot of principal component analysis of combined data on all water samples.

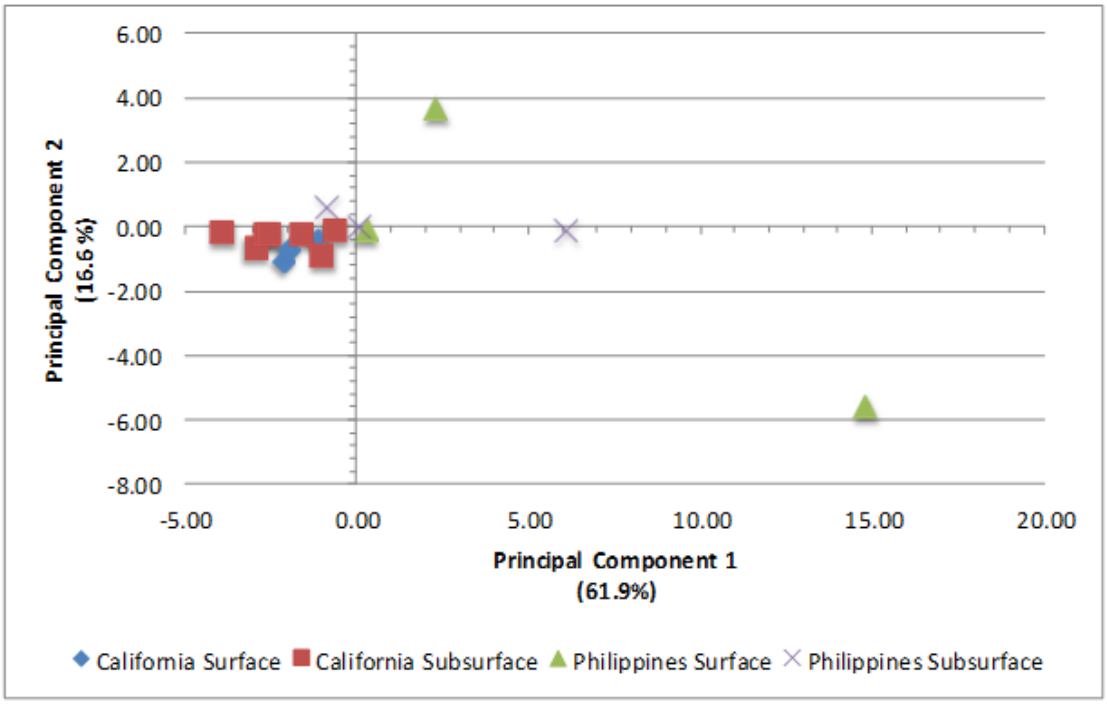

Figure 10. Score plots for principal component analysis spread of sites in relation to carbon utilization for all water samples.

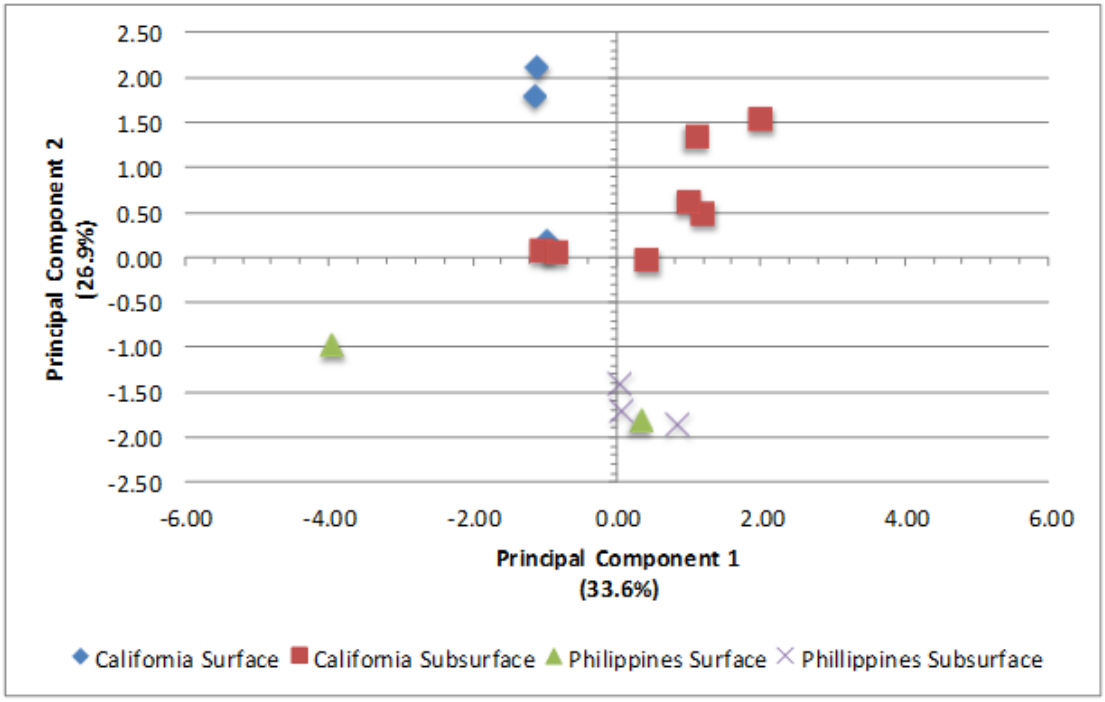

Figure 11. Score plots for principal component analysis spread of sites in relation to environmental data for all water samples.

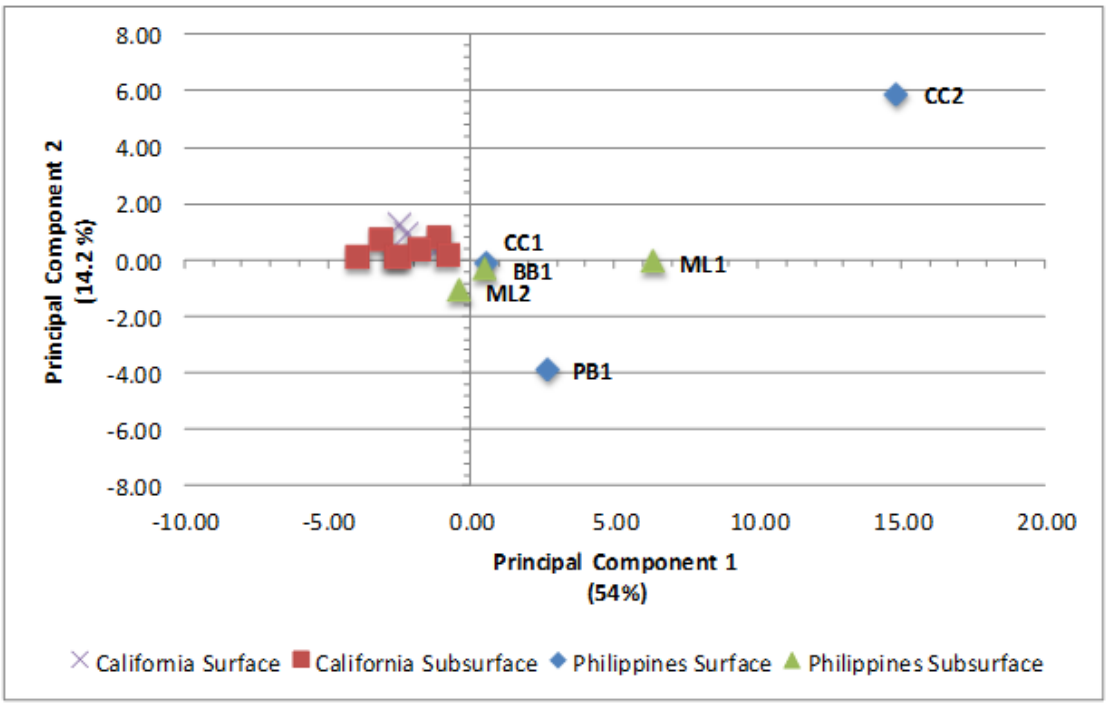

Figure 12. Score plots for principal component analysis spread of sites in relation to all parameters for all water samples.

Guild	Carbon Source	TC-A	TC-B	TC-C	TC-D	TC-E
Amino acids	**L-Arginine**	Yes	Yes	Yes	Yes	Yes
	L-Asparagine	Yes	Yes	Yes	Yes	Yes
	L-Phenylalanine	No	No	No	No	Yes
	L-Serine	Yes	Yes	Yes	Yes	Yes
	L-Threonine	No	Yes	Yes	Yes	Yes
Amines and amides	**Phenylethyl-amine**	Yes	No	Yes	Yes	Yes
	Putrescine	Yes	Yes	Yes	Yes	Yes
Carboxylic acids	**D-Galactonic Acid γ-Lactone**	Yes	Yes	Yes	Yes	Yes
	D-Galacturonic Acid	Yes	Yes	Yes	Yes	Yes
	2-Hydroxy Benzoic Acid	No	No	No	No	No
	4-Hydroxy Benzoic Acid	No	No	No	No	Yes
	γ-Hydroxybutyric Acid	No	No	No	No	Yes
	D-Glucosaminic Acid	Yes	Yes	Yes	Yes	Yes
	Itaconic Acid	Yes	Yes	Yes	Yes	Yes
	glycyl-L-Glutamic Acid	Yes	Yes	Yes	Yes	Yes
	α-Ketobutyric Acid	No	No	Yes	Yes	Yes
	D-Malic Acid	Yes	Yes	Yes	Yes	Yes
Carbohydrates	**β-Methyl-D-Glucoside**	Yes	Yes	Yes	Yes	Yes
	D-Xylose	Yes	Yes	Yes	Yes	Yes
	i-Erythritol	Yes	Yes	Yes	Yes	Yes
	D-Mannitol	Yes	No	Yes	No	Yes
	N-Acetyl-D-Glucosamine	No	No	Yes	Yes	Yes
	D-Cellobiose	Yes	Yes	Yes	Yes	Yes
	α-D-Lactose	Yes	Yes	Yes	Yes	Yes
Miscellaneous	**Pyruvic Acid Methyl Ester**	No	No	No	Yes	Yes
	Glucose-1-Phosphate	Yes	Yes	Yes	Yes	Yes
	D,L-α-Glycerol Phosphate	Yes	Yes	Yes	Yes	Yes
Polymers	**Tween 40**	No	Yes	Yes	Yes	Yes
	Tween 80	Yes	Yes	Yes	Yes	Yes
	α-Cyclodextrin	No	No	No	No	Yes
	Glycogen	Yes	Yes	Yes	Yes	Yes
Control	**Water**	No	No	No	No	No

Table 2. California surface sites carbon utilization patterns from EcoPlate™ experiments. Initial values were determined by calculated the area under the curve per time point from absorption values calculating the average well color density (AWCD). The AWCD greater than zero correspond to a "Yes" response. Values less than Zero correspond to a "No" response.

Guild	Carbon Source	CSW 1,1	CSW 1,4	CSW1,5	OLD CSW	QV1,1	QV1,2	QV1,3
Amino acids	**L-Arginine**	Yes	Yes	Yes	Yes	Yes	Yes	Yes
	L-Asparagine	Yes	Yes	Yes	Yes	Yes	Yes	Yes
	L-Phenylalanine	Yes	Yes	Yes	No	No	No	Yes
	L-Serine	Yes	Yes	Yes	No	Yes	No	Yes
	L-Threonine	Yes	No	Yes	No	Yes	No	Yes
Amines and amides	**Phenylethyl-amine**	Yes	Yes	Yes	Yes	Yes	Yes	Yes
	Putrescine	Yes	Yes	Yes	Yes	Yes	Yes	Yes
Carboxylic acids	**D-Galactonic Acid γ-Lactone**	Yes	Yes	Yes	Yes	Yes	Yes	Yes
	D-Galacturonic Acid	Yes	Yes	Yes	No	Yes	Yes	Yes
	2-Hydroxy Benzoic Acid	No	No	No	No	No	No	No
	4-Hydroxy Benzoic Acid	No	Yes	Yes	No	No	No	Yes
	γ-Hydroxybutyric Acid	Yes	Yes	Yes	No	Yes	Yes	Yes
	D-Glucosaminic Acid	Yes	Yes	Yes	No	Yes	No	Yes
	Itaconic Acid	Yes	Yes	Yes	No	Yes	Yes	Yes
	glycyl-L-Glutamic Acid	Yes	Yes	Yes	No	Yes	No	Yes
	α-Ketobutyric Acid	Yes	Yes	Yes	Yes	Yes	No	Yes
	D-Malic Acid	Yes	Yes	Yes	Yes	Yes	No	Yes
Carbohydrates	**β-Methyl-D-Glucoside**	No	No	No	Yes	Yes	Yes	No
	D-Xylose	Yes	Yes	Yes	Yes	Yes	Yes	Yes
	i-Erythritol	No	No	No	No	No	No	No
	D-Mannitol	No	Yes	Yes	No	No	Yes	No
	N-Acetyl-D-Glucosamine	Yes	No	No	No	Yes	Yes	Yes
	D-Cellobiose	Yes	Yes	Yes	Yes	Yes	Yes	Yes
	α-D-Lactose	Yes	Yes	Yes	Yes	Yes	No	Yes
Miscellaneous	**Pyruvic Acid Methyl Ester**	No	Yes	Yes	No	Yes	Yes	No
	Glucose-1-Phosphate	Yes	No	Yes	Yes	Yes	No	Yes
	D,L-α-Glycerol Phosphate	Yes	Yes	Yes	Yes	Yes	No	Yes
Polymers	**Tween 40**	Yes	Yes	Yes	Yes	Yes	Yes	Yes
	Tween 80	Yes	Yes	Yes	No	Yes	Yes	Yes
	α-Cyclodextrin	Yes	Yes	No	No	Yes	No	Yes
	Glycogen	Yes	Yes	Yes	No	Yes	Yes	Yes
Control	**Water**	No	No	No	No	No	No	No

Table 3. California Subsurface sites carbon utilization patterns from EcoPlate™ experiments. Initial values were determined by calculated the area under the curve per time point from absorption values calculating the average well color density (AWCD). The AWCD greater than zero correspond to a "Yes" response. Values less than Zero correspond to a "No" response.

		Surface			Subsurface		
Guild	**Carbon Source**	**CC1**	**CC2**	**PB 1**	**ML 1**	**ML 2**	**BB1**
Amino acids	**L-Arginine**	Yes	Yes	Yes	Yes	Yes	Yes
	L-Asparagine	Yes	Yes	Yes	Yes	Yes	Yes
	L-Phenylalanine	Yes	Yes	Yes	Yes	Yes	Yes
	L-Serine	Yes	Yes	Yes	No	Yes	Yes
	L-Threonine	Yes	Yes	Yes	No	Yes	Yes
Amines and amides	**Phenylethyl-amine**	Yes	Yes	Yes	Yes	Yes	Yes
	Putrescine	Yes	Yes	Yes	Yes	Yes	Yes
Carboxylic acids	**D-Galactonic Acid γ-Lactone**	Yes	Yes	Yes	No	Yes	Yes
	D-Galacturonic Acid	Yes	Yes	No	No	No	No
	2-Hydroxy Benzoic Acid	No	No	No	No	No	No
	4-Hydroxy Benzoic Acid	Yes	Yes	No	Yes	No	Yes
	γ-Hydroxybutyric Acid	Yes	Yes	Yes	Yes	Yes	Yes
	D-Glucosaminic Acid	Yes	Yes	Yes	Yes	Yes	Yes
	Itaconic Acid	Yes	Yes	Yes	Yes	Yes	Yes
	glycyl-L-Glutamic Acid	Yes	Yes	Yes	Yes	Yes	Yes
	α-Ketobutyric Acid	Yes	Yes	Yes	Yes	Yes	Yes
	D-Malic Acid	Yes	Yes	Yes	Yes	Yes	Yes
Carbohydrates	**β-Methyl-D-Glucoside**	Yes	Yes	No	No	No	No
	D-Xylose	Yes	Yes	Yes	Yes	Yes	Yes
	i-Erythritol	Yes	No	No	No	No	No
	D-Mannitol	Yes	Yes	No	No	No	No
	N-Acetyl-D-Glucosamine	Yes	Yes	Yes	No	No	Yes
	D-Cellobiose	Yes	Yes	Yes	Yes	Yes	Yes
	α-D-Lactose	Yes	Yes	Yes	Yes	Yes	Yes
Miscellaneous	**Pyruvic Acid Methyl Ester**	Yes	Yes	No	Yes	No	Yes
	Glucose-1-Phosphate	Yes	Yes	Yes	Yes	Yes	Yes
	D,L-α-Glycerol Phosphate	Yes	Yes	Yes	Yes	Yes	Yes
Polymers	**Tween 40**	Yes	Yes	Yes	Yes	Yes	Yes
	Tween 80	Yes	Yes	Yes	Yes	Yes	Yes
	α-Cyclodextrin	Yes	Yes	Yes	No	Yes	Yes
	Glycogen	Yes	Yes	Yes	Yes	Yes	Yes
Control	**Water**	No	No	No	No	No	No

Table 4. Philippines surface and subsurface sites carbon utilization patterns from EcoPlate™ experiments. Initial values were determined by the area under the curve per time point from absorption values calculating the average well color density (AWCD). The AWCD greater than zero correspond to a "Yes" response. Values less than Zero correspond to a "No" response.

Site ID	Temp (°C)	Cond. (mS/cm)	DO (%)	pH	ORP (mv)	Ca/Mg	Depth (m)	Lithology
CSW 1-1	18.2	5.09	1.5	12.2	-196	6.6	19.5	Serpentine gravel in clay
CSW 1-2	22.1	3.63	6.8	9.1	-32	19.5	19.2	Serpentine gravel in clay
CSW 1-3	16.6	4.42	2.6	10.1	-70	5.3	23.2	Serpentine rich altered mafic rock
CSW 1-4	17.5	1.70	2.7	7.8	-23	0.5	8.8	Serpentine gravel in clay
CSW 1-5	16.4	4.17	0.6	9.6	-110	6.4	27.4	Altered mafic rock
OLD CSW	28.8	11.34	2.0	9.6	-295	20.4	>30m	Altered mafic rock
QV 1-1	17.6	2.09	1.3	11.2	-40	18.5	23	Magnetite bearing clay with albite
QV 1-2	17.5	1.63	0.5	7.9	-33	6.9	14.9	Magnetite bearing serpentine with clays, albite, and quartz
QV 1-3	16.9	3.10	0.5	9.4	-52	99.2	34.6	Altered mafic rock
TC A	22.6	5.72	19.3	8.1	-22	0.2	surface	Travertine
TC C	22.2	3.79	24.4	8.3	-29	0.2	surface	Travertine
TC E	23.8	3.53	21.0	8.6	-19	0.1	surface	Travertine
CC1	33.8	0.31	62.5	10.8	-245	30.3	surface	Travertine
CC2	32.6	0.27	0.5	10.2	-213	8.6	surface	Travertine
PB 1	30.4	0.34	0.6	10.5	-115	14	surface	Travertine
ML1	34.4	0.39	0.3	10.9	-460	5.8	30-40	Gabbro
ML2	34.4	0.39	0.1	10.8	-425	5.9	30-40	Gabbro
BB1	29.7	0.45	0.0	9.2	-108	0.5	200	Altered pillow basalts

Table 5. Environmental data of all sites. Cores were drilled for Sites CSW 1-1 and QV 1-1, because of close proximity to these wells other CSW and QV wells are correlated to the respective rock sequences (Cardace et al., 2013). Philippines sites are related here to bedrock geology known for the region (Aurelio and Pena, 2010).

APPENDIX

Guild	Carbon Source	PC 1	PC 2	PC 3	PC 4	PC 5	PC 6
Amino acids	**L-Arginine**	0.17	0.23	-0.10	-0.13	-0.15	0.33
	L-Asparagine	0.20	0.17	-0.15	0.05	-0.04	0.07
	L-Phenylalanine	0.14	0.34	-0.11	0.12	0.05	-0.05
	L-Serine	0.21	-0.02	0.06	0.15	-0.01	0.03
	L-Threonine	0.20	0.07	0.19	0.23	0.12	-0.18
Amines and amides	**Phenylethyl-amine**	0.18	0.17	0.23	-0.04	-0.16	-0.03
	Putrescine	0.21	0.16	0.02	-0.09	-0.11	0.15
Carboxylic acids	**D-Galactonic Acid γ-Lactone**	0.18	-0.25	-0.05	0.00	0.00	0.14
	D-Galacturonic Acid	0.16	-0.25	-0.15	-0.01	0.22	0.16
	2-Hydroxy Benzoic Acid	-0.14	0.00	0.30	0.41	0.38	0.20
	4-Hydroxy Benzoic Acid	0.17	0.20	-0.17	0.30	0.13	-0.12
	γ-Hydroxybutyric Acid	0.07	0.12	0.13	-0.57	0.60	-0.10
	D-Glucosaminic Acid	0.20	-0.19	0.08	0.00	-0.02	-0.07
	Itaconic Acid	0.17	-0.14	-0.12	0.04	0.38	-0.08
	glycyl-L-Glutamic Acid	0.21	-0.07	0.17	-0.07	-0.02	-0.08
	α-Ketobutyric Acid	0.10	0.15	0.49	0.16	-0.06	0.13
	D-Malic Acid	0.22	-0.03	0.02	0.08	0.01	-0.19
Carbohydrates	**β-Methyl-D-Glucoside**	0.18	-0.25	-0.12	-0.07	-0.02	-0.11
	D-Xylose	0.20	-0.05	0.18	-0.20	-0.18	-0.01
	i-Erythritol	0.14	-0.27	-0.14	0.21	-0.05	-0.23
	D-Mannitol	0.14	-0.22	-0.11	0.06	0.09	0.70
	N-Acetyl-D-Glucosamine	0.21	0.01	-0.13	0.18	0.03	-0.16
	D-Cellobiose	0.20	-0.22	-0.02	-0.06	-0.07	-0.09
	α-D-Lactose	0.18	-0.03	0.36	-0.08	-0.22	0.00
Miscellaneous	**Pyruvic Acid Methyl Ester**	0.19	0.14	-0.22	-0.13	-0.10	0.16
	Glucose-1-Phosphate	0.20	-0.22	-0.01	-0.02	-0.04	-0.09
	D,L-α-Glycerol Phosphate	0.21	-0.10	0.19	-0.07	-0.05	0.01
Polymers	**Tween 40**	0.16	0.27	-0.18	0.13	0.03	-0.02
	Tween 80	0.18	0.23	-0.20	0.01	-0.01	0.00
	α-Cyclodextrin	0.18	0.05	0.19	0.15	0.25	0.12
	Glycogen	0.18	0.19	-0.02	-0.24	0.17	-0.06

Table A1. Principal component analysis loading values for vector plot of carbon utilization only.

Environmental Parameter	PC1	PC 2	PC 3	PC4	PC 5	PC 6
Temp (°C)	-0.12	-0.57	0.09	0.81	-0.03	0.04
Cond.(mS/cm)	0.18	0.62	0.15	0.42	-0.60	0.15
% DO	-0.26	0.49	-0.46	0.38	0.58	0.01
pH	0.62	-0.13	-0.28	0.00	0.15	0.70
ORP (mv)	-0.62	0.04	0.33	-0.13	0.02	0.69
Ca/Mg	0.33	0.17	0.75	0.11	0.53	-0.07

Table A2. Principal component analysis loading values for vector plot of environmental parameters only.

Guild	Environmental Parameter	PC 1	PC 2	PC3	PC 4	PC 5	PC 6
Amino acids	**L-Arginine**	0.17	-0.22	-0.11	0.04	-0.10	0.09
	L-Asparagine	0.20	-0.15	-0.17	0.05	0.04	0.01
	L-Phenylalanine	0.13	-0.32	-0.14	0.06	0.12	-0.02
	L-Serine	0.21	0.03	0.02	0.02	0.14	0.01
	L-Threonine	0.19	-0.06	0.15	0.11	0.22	-0.04
Amines and amides	**Phenylethyl-amine**	0.18	-0.17	0.18	-0.03	0.06	0.15
	Putrescine	0.20	-0.15	0.00	0.00	-0.03	0.09
Carboxylic acids	**D-Galactonic Acid γ-Lactone**	0.18	0.25	-0.02	0.03	-0.04	-0.06
	D-Galacturonic Acid	0.16	0.26	-0.12	-0.05	-0.01	-0.21
	2-Hydroxy Benzoic Acid	-0.14	-0.01	0.25	0.06	0.37	-0.29
	4-Hydroxy Benzoic Acid	0.17	-0.18	-0.20	0.11	0.22	-0.10
	γ-Hydroxybutyric Acid	0.07	-0.13	0.16	-0.26	-0.35	-0.31
	D-Glucosaminic Acid	0.19	0.20	0.08	-0.02	0.03	0.02
	Itaconic Acid	0.16	0.15	-0.13	-0.07	0.07	-0.24
	glycyl-L-Glutamic Acid	0.20	0.07	0.17	0.00	-0.01	0.05
	α-Ketobutyric Acid	0.11	-0.15	0.41	0.02	0.22	0.07
	D-Malic Acid	0.22	0.04	0.00	0.06	0.07	0.03
Carbohydrates	**β-Methyl-D-Glucoside**	0.17	0.25	-0.10	-0.04	-0.06	0.01
	D-Xylose	0.20	0.05	0.17	-0.02	-0.14	0.15
	i-Erythritol	0.14	0.29	-0.15	0.08	0.12	0.10
	D-Mannitol	0.14	0.23	-0.08	0.05	-0.03	-0.23
	N-Acetyl-D-Glucosamine	0.21	0.01	-0.15	0.06	0.13	-0.02
	D-Cellobiose	0.19	0.22	-0.01	-0.03	-0.04	0.05
	α-D-Lactose	0.18	0.03	0.32	0.01	0.00	0.22
Miscellaneous	**Pyruvic Acid Methyl Ester**	0.19	-0.13	-0.22	-0.05	-0.09	0.04
	Glucose-1-Phosphate	0.19	0.22	0.00	-0.03	0.00	0.05
	D,L-α-Glycerol Phosphate	0.21	0.10	0.17	-0.02	-0.01	0.07
Polymers	**Tween 40**	0.16	-0.25	-0.21	0.03	0.11	-0.03
	Tween 80	0.18	-0.22	-0.21	0.02	0.02	0.01
	α-Cyclodextrin	0.18	-0.05	0.17	-0.02	0.16	-0.26
	Glycogen	0.18	-0.19	-0.02	-0.04	-0.12	-0.13
Environmental Parameter	**Temp (°C)**	0.14	-0.08	0.21	0.02	-0.30	0.34
	Cond. (mS/cm)	-0.12	0.10	-0.15	-0.04	0.35	0.37
	% DO	-0.07	0.08	-0.19	0.32	-0.05	0.36
	pH	0.02	-0.01	-0.12	-0.58	0.06	0.16
	ORP (mv)	-0.01	0.03	0.11	0.60	-0.05	-0.12
	Ca/Mg	-0.02	0.04	0.09	-0.24	0.43	0.08

Table A3. Principal component analysis loading values for vector plot of combined carbon source and environmental data.

Score Plot Carbon Sources		
	PC 1	**PC 2**
CSW1,1	-3.91	-0.15
CSW 1,4	-1.03	-0.86
CSW1,5	-0.65	-0.13
OLD CSW	-2.98	-0.63
QV1,1	-2.70	-0.25
QV1,2	-2.55	-0.21
QV1,3	-1.63	-0.21
TC-A	-2.19	-1.05
TC-C	-1.97	-0.74
TC-E	-1.17	-0.43
CC1	0.25	-0.10
CC2	14.76	-5.58
PB 1	2.29	3.66
ML 1	6.06	-0.12
ML 2	-0.90	0.61
BB1	0.12	0.02

Table A4. Principal component analysis loading values for score plot of carbon sources only.

Score Plot Environmental Parameters		
Site ID	**PC 1**	**PC 2**
CSW1,1	1.19	0.49
CSW 1,4	-1.04	0.08
CSW1,5	1.00	0.62
OLD CSW	1.11	1.35
QV1,1	0.40	-0.02
QV1,2	-0.86	0.06
QV1,3	1.98	1.53
TC-A	-1.12	2.12
TC-C	-1.17	1.80
TC-E	-0.95	0.19
CC1	-3.94	-0.97
CC2	0.34	-1.81
PB 1	0.97	-1.86
ML 1	0.05	-1.70
ML 2	0.83	-1.85
BB1	0.02	-1.40

Table A5. Principal component analysis loading values for score plot of environmental parameters only.

Score Plot All Parameters		
SITE ID	**PC 1**	**PC 2**
CSW1,1	-3.98	0.13
CSW 1,4	-1.08	0.84
CSW1,5	-0.81	0.17
OLD CSW	-3.17	0.74
QV1,1	-2.68	0.16
QV1,2	-2.56	0.14
QV1,3	-1.88	0.40
TC-A	-2.55	1.32
TC-C	-2.25	0.97
TC-E	-1.18	0.41
CC1	0.48	-0.09
CC2	14.78	5.89
PB 1	2.68	-3.85
ML 1	6.32	-0.03
ML 2	-0.45	-1.06
BB1	0.42	-0.29

Table A6. Principal component analysis loading values for score plot of combined carbon source and environmental data.

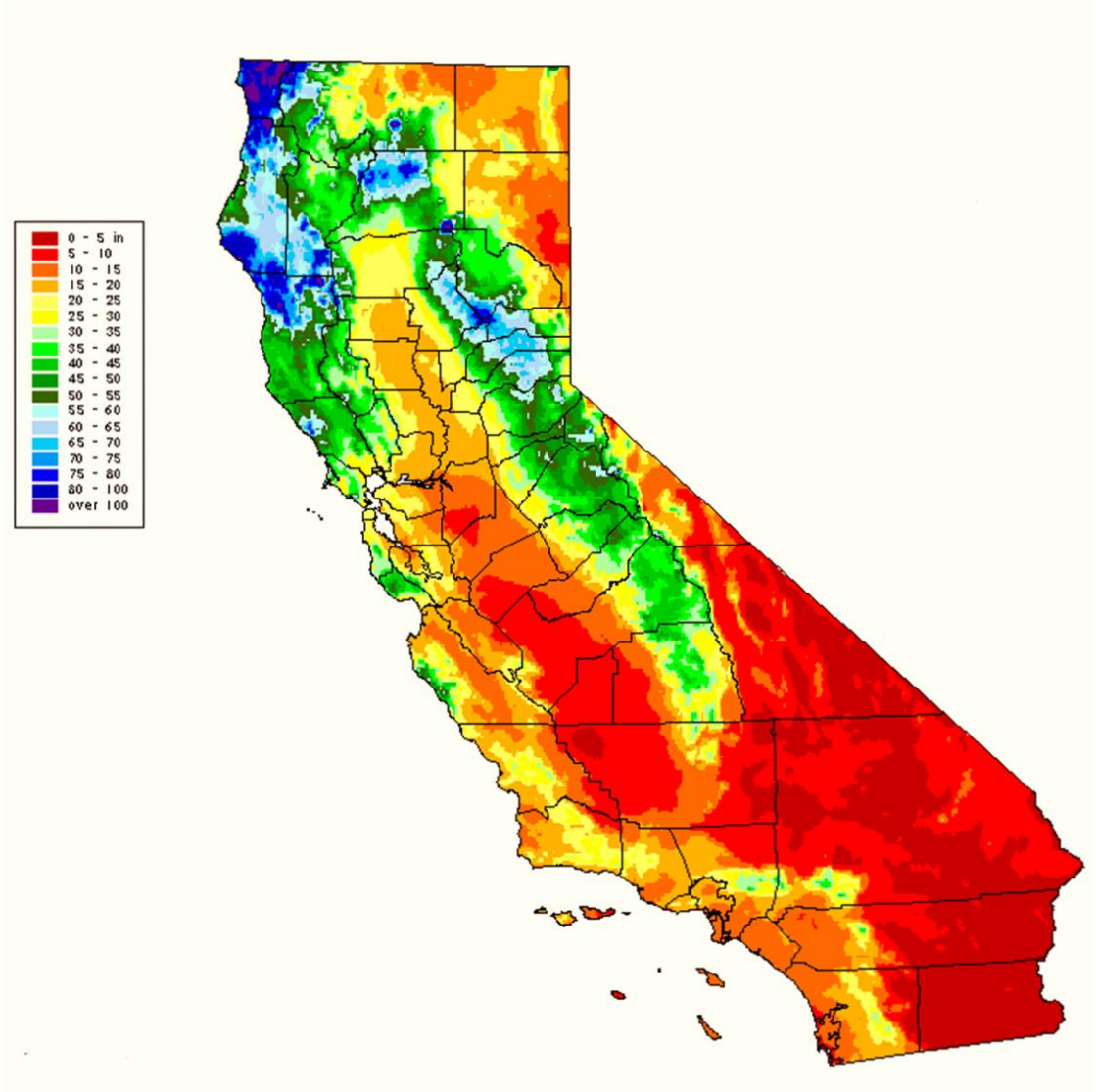

Figure A1. Average annual precipitation map (in inches) for California; 1995 data are shown. (WRCC, 2014).

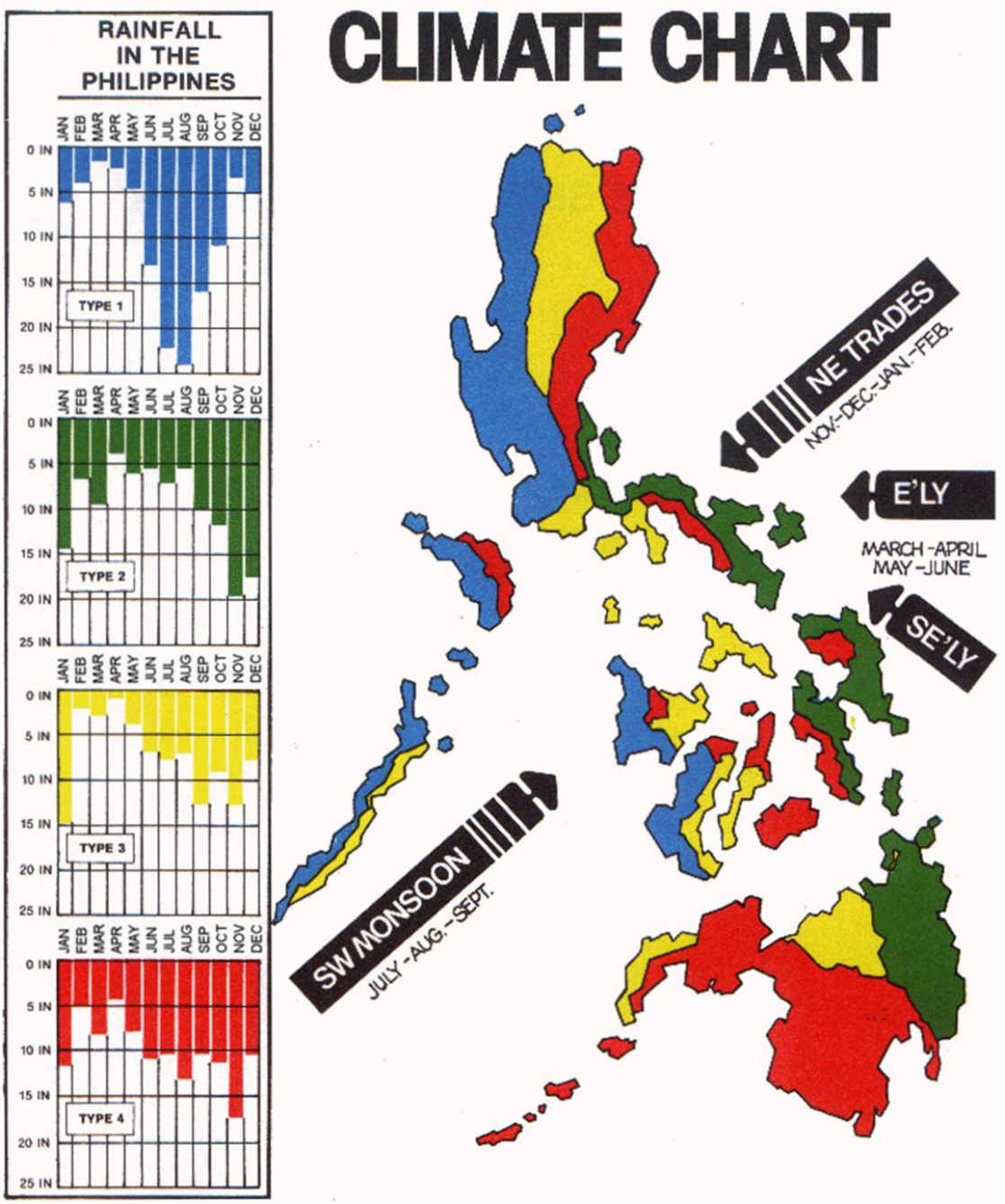

Figure A2. Philippines precipitation charts (in inches) overlain by monsoon map. (Padua, 1997).